



OPEN ACCESS

EDITED BY

Selvaraj Kandasamy,
Central University of Tamil Nadu, India

REVIEWED BY

Sudheesh Valliyodan,
Central University of Kerala, India
Wei-dong Zhai,
Southern Marine Science and Engineering
Guangdong Laboratory (Zhuhai), China

*CORRESPONDENCE

Jia-Jang Hung

✉ hungjj@mail.nsysu.edu.tw

RECEIVED 07 February 2024

ACCEPTED 13 May 2024

PUBLISHED 28 May 2024

CITATION

Hung J-J, Tsai S-H, Lin Y-H and
Hsiang Z-Y (2024) Characterizing dissolved
inorganic and organic nutrients in the
oligotrophic Kuroshio Current off
eastern Taiwan during warm seasons.
Front. Mar. Sci. 11:1383244.
doi: 10.3389/fmars.2024.1383244

COPYRIGHT

© 2024 Hung, Tsai, Lin and Hsiang. This is an
open-access article distributed under the terms
of the [Creative Commons Attribution License
\(CC BY\)](https://creativecommons.org/licenses/by/4.0/). The use, distribution or reproduction
in other forums is permitted, provided the
original author(s) and the copyright owner(s)
are credited and that the original publication
in this journal is cited, in accordance with
accepted academic practice. No use,
distribution or reproduction is permitted
which does not comply with these terms.

Characterizing dissolved inorganic and organic nutrients in the oligotrophic Kuroshio Current off eastern Taiwan during warm seasons

Jia-Jang Hung^{1*}, Sheng-Hsian Tsai^{1,2}, Yen-Hui Lin¹
and Zhi-Ying Hsiang¹

¹Department of Oceanography, National Sun Yat-Sen University, Kaohsiung, Taiwan,

²SGS Taiwan Ltd, Kaohsiung, Taiwan

This study conducted sensitive and precise analyses of dissolved organic nitrogen (DON) and dissolved organic phosphorus (DOP) concentrations and trace concentrations of nitrate and nitrite (N+N) and soluble reactive phosphorus (SRP) in seawater. The methods were applied to investigate the distributions and controls of N+N, SRP, DON, and DOP in the oligotrophic Kuroshio Current (KC) area off eastern Taiwan during warm seasons. The water in the studied area was classified into four major types: typical Kuroshio water (KW), KW influenced by the East China Sea water, KC influenced by the South China Sea (SCS) water, and KW influenced by the SCS water and river plumes, which is confined to the coastal zone. Nutrient distributions in KC revealed very low N+N (0.002–0.40 μM) and SRP (0.015–0.125 μM) concentrations but high DON (<8 μM) and DOP (<0.3 μM) concentrations above the nutricline depth, which accounted for >80% of TDN and TDP, respectively; these concentrations can primarily be attributed to strong, permanent surface stratification. Among the water types, KW had the lowest N+N, SRP, DON, and DOP concentrations but greatest chlorophyll maximum depth and nutricline depth, except for in locations influenced by island-induced upwelling. The concentrations of all nutrients increased by various degrees in the other water types, which was attributed to the exchange and mixing of different water masses and coastal uplift of subsurface waters. KW was not only highly oligotrophic but also N+N-limited reflected from very low [N+N]/[SRP] ratio (0.02–0.15) in the mixed layer (ML). Overall, the N+N limitation and high nitrate anomaly value (N^* : $2.47 \pm 0.16 \mu\text{M}$) above the nutricline depth strongly indicate prevailing N_2 fixation at the surface of KW. Very high DON/DOP ratio in KW (16.9–69.1) probably resulted from the release of N-rich organic nutrients from phytoplankton including N_2 fixers at the surface and faster recycling of DOP than DON in deep waters. Persistent coastal uplift of

subsurface water occurs everywhere over the shore-side region of the KC, resulting in increasing surface concentrations of nutrients and chlorophyll *a*. Overall, the aforementioned physical and biogeochemical processes determined the upper-ocean distributions of nutrient species in warm seasons.

KEYWORDS

nitrate and nitrite, dissolved organic nitrogen, dissolved organic phosphorus, N+N-limitation, N₂ fixation, Kuroshio Current

1 Introduction

The Kuroshio Current (KC), a strong western boundary current, not only has a significant impact on the climate of East Asia and the Northwest Pacific (Komatsu and Hiroe, 2019; Kodama et al., 2021), but also plays an important role in the global climate (Hu et al., 2015; Wan et al., 2023). The KC originates from the Pacific North Equatorial Current which bifurcates at the east coast of Luzon, from where the KC flows northwardly along the east coasts of Taiwan and reaches the south coast of Japan (Nitani, 1972; Qu and Lukas, 2003). In the Bashi Channel, a branch of Kuroshio surface and bottom currents flow into the northern South China Sea (SCS). This branch is accompanied by an intermediate water outflow from the northern SCS into the West Philippine Sea; the outflow results in strong mixing between the SCS water (SCSW) and Kuroshio water (KW; Shaw, 1991; Chen and Wang, 1998; Chou et al., 2007; Nan et al., 2015). The KC flows along the east coast of Taiwan and exhibits surface waters characterized by relatively high temperatures and salinity and low amounts of nutrients; however, the main axis of the KC is subject to seasonal variability that can strongly affect surface hydro-biological conditions and ecosystems (Hsin et al., 2013; Chen et al., 2017; Komatsu and Hiroe, 2019; Saito, 2019; Kodama et al., 2021). Thus, the KC has surface waters with relatively low primary productivity but abundant biota and fish populations in regions with an abrupt change in topography (Chiu and Huang, 1994; Wang and Lee, 2019). This enhanced productivity may be derived from a “nutrient stream” formed in the Kuroshio subsurface waters; this stream flows northward, causing upwelling and an increase in productivity in the northeast of Taiwan where the KC encounters the shelf of the East China Sea (Guo et al., 2013; Chen et al., 2017, 2021).

In warm oligotrophic ocean waters such as the upper waters of the KC, where the river inputs are small and nitrate and phosphate are scarce, the growth of marine phytoplankton is commonly restricted by the limited availability of nitrogen or phosphorus (Graziano et al., 1996; Mills et al., 2004; Moore et al., 2013; Browning and Moore, 2023). Although previous studies have pointed out the important contribution of atmospheric deposition of dissolved inorganic nitrogen to biological productivity in the SCS

(Gao et al., 2020), the East China Sea (Zhang et al., 2010; Jin et al., 2024), and the North Pacific Ocean (Kim et al., 2014), it remains unclear at the current stage if the atmospheric deposition provides significant impacts on the distribution of nutrient in the KC. Oligotrophic oceans have large pools of dissolved organic nitrogen (DON) and phosphorus (DOP) that may become sources of nutrients supporting phytoplankton growth and sustaining ecosystem functioning through autotrophic and heterotrophic uptake and decomposition, despite the DON and DOP are mainly derived from phytoplankton release or derived through zooplankton’s sloppy feeding (Jackson and Williams, 1985; Abell et al., 2000; Bronk and Ward, 2000; Hansell and Feely, 2000; Berman and Bronk, 2003; Raimbault et al., 2008; Lomas et al., 2010; Karl and Björkman, 2015; Sarma et al., 2019). In an upper water column characterized by a strong thermal stratification, nutrients are restricted to sunlit surface waters; hence, phytoplankton may seek alternative ways to acquire nitrogen and phosphorus for growth. Marine nitrogen fixation is a crucial process in which abundant nitrogen in the atmosphere is used to convert dissolved N₂ into bioavailable ammonia, particularly in oligotrophic oceans (Capone and Carpenter, 1982; Capone et al., 1997; Gruber and Sarmiento, 1997; Deutsch et al., 2001; Wang et al., 2019; Zehr and Capone, 2020). Previous studies have reported that N₂ fixation can release and accumulate DON that is apparently involved in nitrogen cycling and that enhances carbon sequestration (Karl et al., 1997; Ohlendieck et al., 2000; Sipler and Bronk, 2015). Particular locations of the KC contain abundant nitrogen fixers and have a high rate of nitrogen fixation, thus supplying additional nitrogen to the ocean in summer (Marumo and Asaoka, 1974; Liu et al., 1996; Chen et al., 2014). Iron supply may be critical to the growth of phytoplankton and nitrogen fixers in oligotrophic oceans (Grabowski et al., 2008; Isada et al., 2019; Sato et al., 2021).

Several studies on the role of DOP in sustaining N₂ fixation have indicated that in phosphate-depleted oligotrophic regions, nitrogen-fixing phytoplankton uses organic forms of phosphorus as an alternative source of phosphorus through DOP remineralization or direct consumption (Dyhrman et al., 2006; Palter et al., 2011; Filella et al., 2022). This is crucial because the concentrations of soluble reactive phosphorus (SRP) in the tropical and subtropical North

Atlantic Ocean are too low to sustain *Trichodesmium* growth (Sohm and Capone, 2006) and molecular analyses have confirmed the ability of *Trichodesmium* to use DOP for N₂ fixation (Dyhrman et al., 2006). Liang et al. (2022) reported that DOP as a dual role in the surface waters of the ocean; fueling primary production and nitrogen fixation, particularly in oligotrophic gyres. They also proposed that phosphate and iron stress, which may limit N₂ fixation, can control the global distribution of DOP. Nevertheless, the role of DOP as an alternative phosphorus source to support nitrogen fixation or primary productivity in the KC remains unclear.

To explore the oceanic roles, processes, and function of DON and DOP, reliable methods for measuring nitrate and nitrite (N+N), SRP, DON, and DOP concentrations are necessary to obtain a clearer understanding of the nutrient biogeochemistry in the upper waters of nutrient-depleted oceans. Quantifying N+N and SRP concentrations in N- and P-depleted oceans is challenging because these concentrations are usually excessively low (nanomolar levels) to be precisely determined using conventional nutrient analyses (Garside, 1982; Karl and Tien, 1992). In addition, the determination of DON and DOP relies heavily on the precise measurement of N+N and SRP. Because physical and biogeochemical studies have focused on regions downstream of the KC or on the limited upstream region connected to the SCS (Chou et al., 2007; Guo et al., 2012; Komatsu and Hiroe, 2019; Saito, 2019; Chen et al., 2021; Joh et al., 2021; Lai et al., 2021), the current understanding of the roles of dissolved inorganic and organic nutrients in the KW off the east coast of Taiwan is relatively limited. Accordingly, to address these knowledge gaps, we attempted to reliably analyze dissolved inorganic and organic nitrogen and phosphorus and employed promising methods to study the distributions and biogeochemical dynamics of inorganic and organic nutrients in the Kuroshio system. Hence, this study not only presents a reliable evaluation of inorganic and organic nutrient pools but also increases the understanding of processes that influence the distributions and dynamics of inorganic and organic nutrients in the Kuroshio upstream.

2 Materials and methods

2.1 Study area and sampling locations

This study employed seawater samples collected from one major scientific cruise (NCOR-JHS, May 22–June 03/2006) that conducted sampling across the entire KC area off eastern Taiwan (Stations ST01–ST41) and those collected from two minor scientific cruises (ORIII-CR1217, April 21–24/2007, and ORIII-CR1234, July 7–10/2007) that conducted sampling in only the southern zones of the KC. The sampling stations and their locations and depths are shown in Table 1 and Figure 1. Because of the high intensity of island–continent collisions, the topography of the seafloor across the KC characterized by an abrupt drop from the nearshore waters to depths greater than 3000 m within a short distance. Most of the sampling stations were noted to be located in deep-water zones (Figure 1). Seawater samples were collected using clean 10-L Niskin bottles mounted on a Rosette attached with CTD. The CTD (SBE 9 CTD; Sea-Bird Electronics, USA) and attached probes were used to record temperature (*T*), salinity (*S*), fluorescence (*F*), and transmission data for a water column. Surface and subsurface irradiance was measured using a photosynthetically active radiation sensor (OSP2001, Biospherical Instruments, San Diego, CA, USA). The euphotic depth was defined as the depth at which the light intensity was 1% of that at the surface. The water samples were collected at depths of 5–600 m, whereas the CTD data were recorded at depths of up to 1000 m; however, the data obtained at stations ST26 and ST28 were recorded at depths of up to 2000 m. The mixed layer depth (MLD) was estimated from the difference in potential density (<0.125 kg m⁻³) between the ocean surface and the bottom of the mixed layer (Monterey and Levitus, 1997). The concentration of chlorophyll *a* (Chl-*a*) was determined from the fluorescence data ($F = -0.007 + 0.317\text{Chl-}a$), which was calibrated using laboratory Chl-*a* measurements performed before the cruises took place. The collected seawater samples were frozen and brought to a land-based laboratory for further analyses.

TABLE 1 A list of sampling dates, stations, water depths, and locations during the NCOR-JHS (early summer), ORIII-CR1217 (spring), and ORIII-CR1234 (summer) cruises.

| Cruise | Station | Longitude (°E) | Latitude (°N) | Depth (m) | Sampling date |
|----------|---------|----------------|---------------|-----------|---------------|
| NCOR-JHS | ST01 | 122° 05.690 | 25°00.320 | 230 | 05/22/06 |
| | ST02 | 122°29.980 | 24°59.930 | 1460 | 05/22/06 |
| | ST03 | 122°29.990 | 25°29.980 | 436 | 05/22/06 |
| | ST04 | 122°30.248 | 26°00.512 | 106 | 05/22/06 |
| | ST05 | 122°59.936 | 25°59.895 | 95 | 05/23/06 |
| | ST06 | 123°00.090 | 25°44.910 | 316 | 05/23/06 |
| | ST07 | 122°59.996 | 25°30.318 | 776 | 05/23/06 |
| | ST08 | 123°00.257 | 25°15.376 | 1623 | 05/23/06 |
| | ST09 | 123°00.208 | 25°00.407 | 1608 | 05/23/06 |
| | ST010 | 122°30.393 | 24°30.414 | 585 | 05/23/06 |
| | ST011 | 122°00.342 | 24°30.102 | 823 | 05/24/06 |

(Continued)

TABLE 1 Continued

| Cruise | Station | Longitude (°E) | Latitude (°N) | Depth (m) | Sampling date |
|--------------|---------|----------------|---------------|-----------|---------------|
| | ST012 | 121°41.517 | 24°02.132 | 200 | 05/24/06 |
| | ST013 | 122°00.108 | 24°00.169 | 3007 | 05/24/06 |
| | ST014 | 122°29.889 | 24°00.095 | 3623 | 05/24/06 |
| | ST015 | 122°59.726 | 24°00.208 | 1038 | 05/24/06 |
| | ST016 | 123°00.185 | 23°30.195 | 3057 | 05/24/06 |
| | ST017 | 122°30.132 | 23°30.045 | 3241 | 05/25/06 |
| | ST018 | 122°00.342 | 23°30.064 | 4249 | 05/25/06 |
| | ST019 | 121°35.250 | 23°00.382 | 1248 | 05/25/06 |
| | ST020 | 121°30.300 | 23°00.382 | 2016 | 05/25/06 |
| | ST021 | 121°59.711 | 22°59.894 | 4896 | 05/25/06 |
| | ST022 | 122°30.214 | 23°00.031 | 5529 | 05/25/06 |
| | ST023 | 122°57.999 | 22°58.098 | 4964 | 05/26/06 |
| | ST024 | 122°59.973 | 22°30.225 | 3240 | 05/26/06 |
| | ST026 | 122°30.517 | 22°30.016 | 4938 | 05/26/06 |
| | ST028 | 121°59.955 | 22°29.905 | 4912 | 05/27/06 |
| | ST030 | 121°30.661 | 22°30.189 | 2116 | 05/27/06 |
| | ST031 | 121°15.580 | 22°30.396 | 1275 | 5/27/06 |
| | ST032 | 120°59.996 | 22°29.915 | 796 | 05/27/06 |
| | ST033 | 121°00.211 | 22°00.337 | 1301 | 05/28/06 |
| | ST034 | 121°14.870 | 21°59.838 | 1482 | 05/28/06 |
| | ST035 | 121°29.766 | 22°00.014 | 1090 | 05/28/06 |
| | ST036 | 121°45.084 | 21°59.951 | 3477 | 05/28/06 |
| | ST037 | 122°00.086 | 22°00.206 | 4594 | 05/29/06 |
| | ST039 | 122°29.843 | 22°00.192 | 4831 | 05/29/06 |
| | ST041 | 122°59.944 | 22°00.131 | 3149 | 05/29/06 |
| ORIII-CR1217 | K1 | 121°00.075 | 22°09.999 | 1050 | 04/21/07 |
| | K2 | 121°23.639 | 22°10.784 | 1911 | 04/22/07 |
| | K4 | 121°47.061 | 22°09.982 | >3000 | 04/22/07 |
| | K5 | 121°59.869 | 22°09.984 | >3000 | 04/23/07 |
| | U1 | 121°23.112 | 21°55.193 | 2760 | 04/24/07 |
| | U2 | 121°47.127 | 21°54.793 | >3000 | 04/24/07 |
| | U3 | 121°00.218 | 21°54.912 | >3000 | 04/24/07 |
| | U4 | 121°00.401 | 21°54.775 | 1321 | 04/24/07 |
| ORIII-CR1234 | T1 | 121°00.036 | 21°55.019 | >3000 | 07/10/07 |
| | T2 | 121°24.022 | 21°55.012 | 2349 | 07/09/07 |
| | T3 | 121°46.945 | 21°55.109 | >3000 | 07/08/07 |
| | T4 | 122°06.040 | 21°54.982 | >3000 | 07/08/07 |

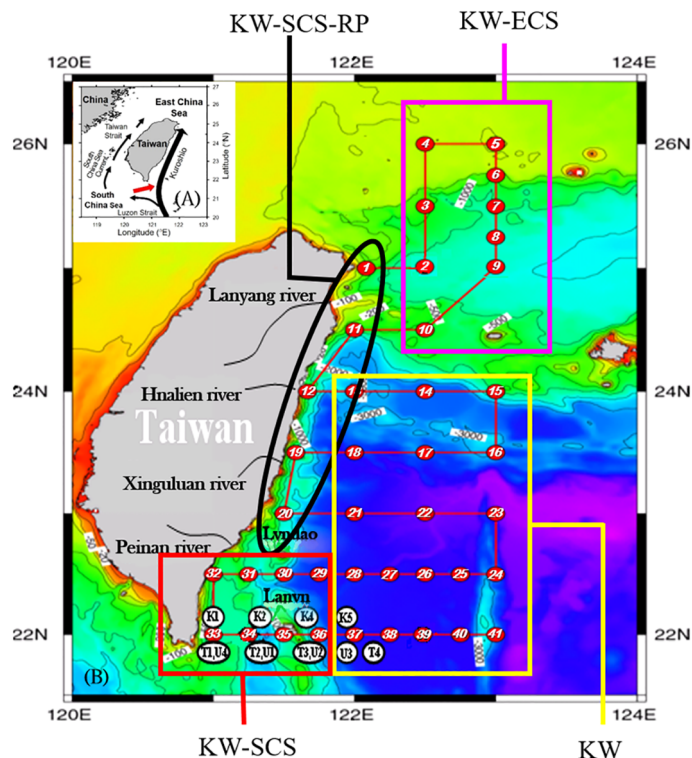
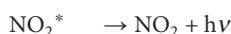
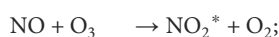
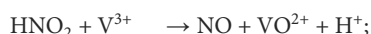
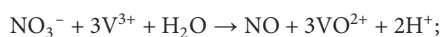


FIGURE 1

Study area and sampling locations during three cruises, NCOR-JHS (May 22–June 3, 2006; ST01–ST41), ORIII-CR1217 (April 21–24, 2007; STK1–STK5 and STU1–STU4), and ORIII-CR1234 (07/08–10/2007; STT1–STT4) in the Kuroshio Current (KC) off the east of Taiwan (B). Four water types in the study area can be identified and grouped in accordance with the $S-\sigma_{\theta}$ relationship at individual stations (Supplementary Figures 1–3); typical Kuroshio water (KW), KW affected by East China Sea water (KW-ECS), KW affected by South China Sea water (KW-SCS), and KW affected by SCS water and river plumes (KW-SCS-RP). Shown are the sampling stations covered by each water type. Insert: Kuroshio surface current and its branch intrusion into the South China Sea (SCS, black arrow) and intermediate-layer outflow from the SCS to the KC (A, red arrow).

2.2 Analyses of trace concentrations of N + N and SRP

The analysis of N+N is principally based on the method of vanadium-reduction proposed by [Braman and Hendrix \(1989\)](#). The vanadium(III) solution was prepared by reduction of acidic 0.10 M solution of vanadyl sulfate ($\text{VOSO}_4 \cdot n\text{H}_2\text{O}$) with Zn under controlling pH below 1.0 to produce dominant $\text{V}(\text{H}_2\text{O})_6^{3+}$ species. The N+N in seawater can be reduced by vanadium(III) to NO that reacts with ozone (O_3) to form NO_2^* and decayed $h\nu$ that was detected by a chemiluminescence analyzer (Antek 7050, Antek Electronic Ltd., USA) according to the following reactions:



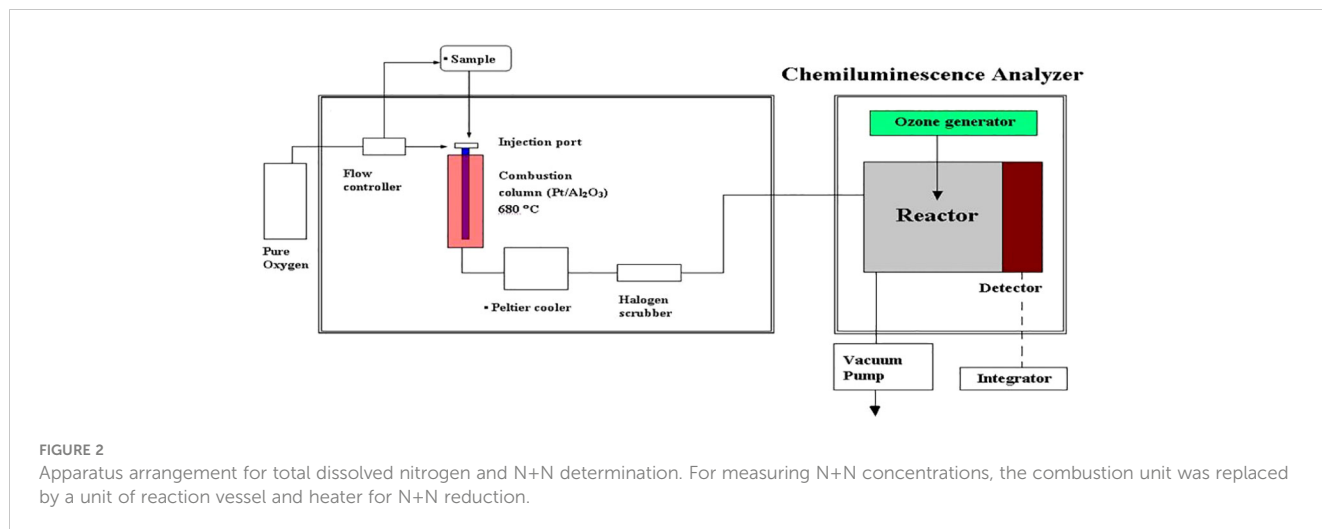
The concentration of N+N in seawater can be determined against N+N standards (1–50 nM; nitrate:nitrite = 4:1) following the steps described in [Figure 2](#) in which the combustion unit (for determining total dissolved nitrogen (TDN)) was replaced by an unit of reaction vessel for N+N reduction warmed by a heater. Thus, N+N and TDN can be measured alternatively by switching the

reaction vessel and combustion unit. The detection limit of N+N can be as low as 0.7 nM, and precision and accuracy of the method are 4.7% (coefficient of variation (C.V.), $n = 12$) and 1.1% (relative error, $n = 6$; based on 90 nM nitrate in certified Seawater Batch #59), respectively ([Table 2](#)).

The SRP concentration of surface samples was determined by the modified MAGIC method ([Tomson-Bullidis and Karl, 1998](#)) with correction for arsenate interference. The precision was estimated as 9.5% (C.V., $n = 12$, [Table 2](#)) by measuring a SCS water sample (mean: 47 nM SRP). However, N+N and SRP concentrations in subsurface and deep waters associated with relatively high concentrations were determined colorimetrically ([Grasshoff et al., 1983](#)) with a UV-Vis spectrophotometer (Hitachi U-3310) equipped with a module of flow injection analysis ([Pai and Riley, 1994](#)). These methods have been established previously ([Hung et al., 2007, 2008, 2021](#)).

2.3 Determination of DON and DOP concentrations

DON was determined by the difference between N+N and TDN that was measured with the chemiluminescence method using a seawater injection and combustion instrument (Shimadzu TOC-



5000) connected to a chemiluminescence detector (Anteck Models 7050) (see Figure 2). The precision and accuracy were 1.7% (C.V., n = 12, by measuring a SCS seawater) and 0.4–1.9% (relative error, n = 6, by measuring a certified DOC SRM sample) (Table 2). DOP was determined by the difference between SRP and total dissolved phosphorus (TDP) that was measured with UV-persulfate oxidation and colorimetric method (Ridal and Moore, 1990). The precision was estimated to be 6.7% (C.V., n = 12) by measuring a SCS seawater sample (Table 2).

2.4 Estimated nutrient inventory

The inventory of N+N, SRP, DON, and DOP within the surface layer (100 m depth) was estimated by the depth-integrated concentration determined in each sampling depth using trapezoidal integration through the 100 m depth.

2.5 Nitrate anomaly

The Nitrate anomaly, N*, was estimated according to the following equation (Deutsch et al., 2001):

$$N^* (\mu M) = N - 16P + 2.90$$

Where N and P are N+N and SRP concentrations, respectively. The constant of 2.90 μM is the global average deficit of nitrate resulted from denitrification.

2.6 Stratification index

The stratification index (SI) was estimated as the difference in potential density (δ_θ) between the upper 10 m (averaged) and 200 m for using as a measure of water column stratification (Lozier et al., 2011; van de Poll et al., 2013). The criterion of SI value for

TABLE 2 Precision and accuracy of analytical methods for determining N+N, SRP, TDN, and TDP concentrations in seawater.

| Parameter | Method | Detection limit (nM) | Precision | | | Accuracy | | |
|-----------------|------------------------------------|----------------------|----------------------|------------|----------|--|----------------------|--------------------|
| | | | Measured conc. (μ M) | Replicates | C.V. (%) | Certified conc. (μ M) | Measured conc. (μ M) | Relative error (%) |
| N+N (low conc.) | V(III) reduction-chemiluminescence | 0.7 | 0.517 ^a | 12 | 4.7 | 0.09 ^b | 0.091 | 1.1 |
| TDN | HTCO-chemiluminescence | 500 | 5.460 ^d | 12 | 1.7 | 33.0 ^c 22.1 ^d | 32.4 21.0 | 1.9 0.4 |
| SRP (low conc.) | MAGIC | 9 | 0.047 ^a | 12 | 9.5 | none | none | none |
| TDP | Persulfate oxidation colorimetry | 91 | 0.353 ^a | 12 | 6.7 | none | none | none |

^aSouth China Sea Water; ^bStandard Seawater Batch NO. 59; ^cDOC CRM Batch 7-2007; ^dDOC CRM Batch 6-2000. C.V., Coefficient of variation. Relative error (%) = | measured-certified | / certified × 100.

non-stratification ($SI < 0.125 \text{ kg m}^{-3}$) was reported by De Boyer Montégut et al. (2004).

3 Results

3.1 Hydrographic conditions

The hydrographic features of each station were determined by measuring T , S , and the density anomaly (σ_θ) in water columns. Table 3 lists the distribution of T , S , and σ_θ in the mixed layer and variations of MLD, deep chlorophyll maximum (DCM) depth, and nitracline depth in four water types. In general, typical KW had highest T and S in the mixed layer and deepest MLD, DCM depth, and nitracline depth; whereas, KW-SCS-RP had lowest T and S in the mixed layer and shallowest MLD, DCM depth, and nitracline depth. The measurements of T , S , and σ_θ in water columns were plotted against the typical T - S relationship for KW and SCSW waters to confirm that the investigated waters were mainly influenced by the KC itself and the mixing between KW and SCSW. The plots of T - S relationships obtained for all stations sampled by the three cruises are illustrated in Supplementary Figures 1–3. Typical KW was characterized by a salinity maximum (34.9) at the surface (200 m), which is typical of the North Pacific Tropical Water, and a salinity minimum (34.2) at 600 m, which is typical of the North Pacific Intermediate Water. At depths below 1500 m, the salinity increased with depth to about 34.7 at the bottom. Consequently, the T - S relationship for KW had an inverted “S” shape. SCSW was characterized by a high temperature and low salinity in the surface layer, high temperature and high salinity in the subsurface layer (~150–250 m), low temperature and low salinity in the intermediate layer (~400–1200 m), and low temperature and high salinity in the deep layer (>1500 m). Accordingly, the properties of the water at each station were primarily determined by assessing the water’s resemblance to either KW or SCSW.

The water at the stations nearest the coast (ST1, ST11, ST12, ST19, and ST20) resembled SCSW with particularly low surface salinity; this water possibly resulted from the mixing of SCSW with KW and freshwater (Supplementary Figure 1). Therefore, the water was classified as KW influenced by SCSW and river plumes (denoted KW-SCS-RP; Figure 1). Moreover, the water at the stations off the northeastern tip of Taiwan (ST02–ST10) resembled SCSW at the surface and KW below the subsurface, possibly resulting from the mixing of the KW, SCSW, and ECSW

(Supplementary Figure 1). Accordingly, the water was classified as KW influenced by ECSW (denoted KW-ECS; Figure 1). The water at the stations near the east-southeast coast (ST29–ST36) mainly resembled SCSW at the surface and KW below the subsurface, possibly resulting from the mixing between SCSW and KW (Supplementary Figure 1). Hence, the water was classified as KW influenced by SCSW (denoted KW-SCS; Figure 1). Finally, the water at the remaining stations (ST 13–ST18, ST21–ST28, and ST37–ST41) mostly resembled KW (Supplementary Figure 1) and was thus classified as typical KW (Figure 1).

The water samples collected in spring (April 21–24, 2007) during the ORIII-CR1217 cruise and in summer (July 7–10, 2007) during the ORIII-CR1234 cruise exhibited properties that resembled those of SCSW and KW (Supplementary Figures 2, 3); thus, the water was determined to be either KW-SCS or KW depending on the variation of the main Kuroshio path, which may cause different conditions for mixing of KW with SCSW.

3.2 Distribution of N+N, SRP, and N/P ratio

Studying the N+N distribution within a depth of 100 m revealed that the N+N concentration ranged from 0.001 μM to 0.892 μM ($0.095 \pm 0.196 \mu\text{M}$) in typical KW, from 0.009 μM to 2.18 μM ($0.250 \pm 0.469 \mu\text{M}$) in KW-SCS, from 0.003 μM to 2.976 μM ($0.628 \pm 0.909 \mu\text{M}$) in KW-ECS, and from 0.02 μM to 6.339 μM ($1.421 \pm 1.871 \mu\text{M}$) in KW-SCS-RP (Table 4; Figure 3A). The depth of 100 m was taken to cover MLD, DCM depth, and nitracline depth, and to systematically compare the magnitude of variables in four water types. Notably, the depth of the thermocline depth is not consistently equivalent to a depth of 100 m. In this study, the N+N concentration was generally highest in KW-SCS-RP and lowest in KW (Figure 3A). Examining the vertical distribution of the N+N concentration revealed that the concentration exhibited little variation above the nitracline depth which is defined as the depth where the nitrate concentration increases below the nutrient depleted upper layer; however, below the nitracline depth, the concentration exhibited a pronounced increase with depth (Figure 4; Supplementary Figure 4A). The nitracline depth was observed to be greater in KW (59–85 m) and KW-SCS (33–69 m) than in KW-SCS-RP (5–43 m) and KW-ECS (41–58 m) (Table 3). Vertical distributions of Chl-*a* revealed the lowest concentration at the surface ($<0.2 \mu\text{g l}^{-1}$) and the maximum concentration at the DCM layer in deep and stratified KW and KW-SCS (Figures 4C, D). The concentration of Chl-*a* was usually elevated at the surface and increased toward the maximum at the DCM layer either in KW-SCS-RP (Figure 4A) or in

TABLE 3 Distributions of temperature, salinity, and density in the mixed layer including various conditions of mixed layer depth (MLD), deep chlorophyll maximum (DCM) depth, and nitracline depth in four water types.

| Water type | T ($^{\circ}\text{C}$) | Salinity | Density (kg m^{-3}) | MLD (m) | DCM depth (m) | Nitracline depth (m) |
|------------|----------------------------|--------------|--------------------------------|---------|---------------|----------------------|
| KW-SCS-RP | 24.85– 28.35 | 33.82– 34.19 | 21.67– 22.49 | 13–23 | 4–49 | 5–43 |
| KW-SCS | 27.70– 28.50 | 34.07– 34.19 | 21.47– 21.82 | 15–43 | 49–80 | 33–69 |
| KW-ECS | 23.63– 28.02 | 33.70– 34.34 | 21.51– 23.25 | 21–47 | 30–69 | 41–58 |
| KW | 27.69– 28.85 | 34.10– 34.55 | 21.66– 22.07 | 15–49 | 51–166 | 59–85 |

TABLE 4 Distributions of N+N, SRP, DON, DOP, N+N/SRP ratio, and DON/DOP ratio in the mixed layer, thermocline, and deep layer in four water types sampled from the NCOR-JHS cruise.

| Water type | Water layer | N+N (μM) | SRP (μM) | DON (μM) | DOP (μM) | N+N/SRP | DON/DOP |
|------------|-------------|-----------------------|-----------------------|-----------------------|-----------------------|-----------|-----------|
| | Mixed layer | 0.02~0.68 | 0.04~0.26 | 4.91~12.6 | 0.23~0.29 | 0.15~3.91 | 21.7~49.9 |
| KW-SCS-RP | Thermocline | 2.10~6.63 | 0.11~0.60 | 4.1~8.13 | 0.20~0.26 | 8.44~21.2 | 26.0~36.7 |
| | Deep layer | 24.7~25.7 | 2.21~2.27 | 2.07~2.31 | 0.03~0.05 | 11.2~16.3 | 40.4~57.8 |
| KW-SCS | Mixed layer | 0.009~0.056 | 0.01~0.07 | 5.68~6.34 | 0.17~0.21 | 0.12~1.10 | 29.0~30.7 |
| | Thermocline | 0.09~2.18 | 0.07~0.18 | 4.96~8.13 | 0.20~0.30 | 1.13~12.2 | 33.5~35.5 |
| | Deep layer | 23.7~26.5 | 1.78~1.86 | 0.97~1.85 | 0.02~0.05 | 12.4~14.5 | 49.6~56.4 |
| KW-ECS | Mixed layer | 0.003~0.024 | 0.04~0.09 | 4.12~7.64 | 0.13~0.29 | 0.05~1.33 | 14.6~29.5 |
| | Thermocline | 0.11~2.98 | 0.06~0.19 | 5.14~8.89 | 0.14~0.25 | 1.56~16.5 | 24.2~40.9 |
| | Deep layer | 26.7~30.8 | 1.75~2.26 | 2.00~2.74 | 0.05~0.10 | 11.8~16.2 | 33.2~59.2 |
| KW | Mixed layer | 0.001~0.009 | 0.01~0.05 | 3.89~7.07 | 0.20~0.25 | 0.02~0.15 | 16.9~27.3 |
| | Thermocline | 0.01~0.52 | 0.04~0.14 | 4.18~7.75 | 0.15~0.30 | 0.24~8.17 | 20.4~39.9 |
| | Deep layer | 17.5~24.3 | 1.35~1.72 | 0.24~1.14 | 0.02~0.08 | 10.3~13.8 | 38.1~69.1 |

KW-ECS influenced by upwelling (Figure 4B). The nitracline depth corresponded to the depth of DCM layer located at the base of the euphotic zone; KW had the deepest DCM, followed by KW-SCS, KW-ECS, and KW-SCS-RP (Figure 4). Hence, the nitracline depth may be regarded as a proxy of the nutrient supply to the upper euphotic layer of the ocean. The DCM is thus generally close to the nitracline depth, but that for KW-SCS is shallower than the nitracline depth. The DCM is also located below the MLD when the surface water is strongly stratified. Overall, the N+N concentration was noted to be higher on the western side of the KC, close to the east coast of Taiwan, than it was on the eastern side of the KC, regardless of the different transects across the KC located on various latitudes (Figure 5).

Assessing the SRP distribution within a depth of 100 m indicated that the SRP concentration ranged from 0.014 to 0.136 μM ($0.054 \pm 0.032 \mu\text{M}$) in typical KW, from 0.014 to 0.180 μM ($0.090 \pm 0.042 \mu\text{M}$) in KW-SCS, from 0.034 to 0.182 μM ($0.089 \pm 0.042 \mu\text{M}$) in KW-ECS, and from 0.040 to 0.359 μM ($0.162 \pm 0.100 \mu\text{M}$) in KW-SCS-RP (Table 4; Figure 3A). The concentration was highest in KW-SCS-RP and lowest in KW. The vertical SRP distribution was similar to the vertical N+N distribution. Specifically, below the nitracline depth, the concentration increased with depth (Figure 6; Supplementary Figure 4B). The nitracline depth and DCM can thus be determined to be closely related (Figure 6).

Examining the distribution of the N+N/SRP ratio within the top 100 m of the water column indicated that the ratio ranged from 0.02 to 8.17 (0.98 ± 1.81) in typical KW, from 0.12 to 13.6 (2.44 ± 3.58) in KW-SCS, from 0.05 to 16.5 (4.82 ± 6.30) in KW-ECS, and from 0.15 to 21.2 (6.61 ± 7.82) in KW-SCS-RP (Table 4). The N/P ratio was highest in KW-SCS-RP and lowest in KW. The ratio generally increased with depth in all four water types. The averaged N/P ratio was determined to be considerably lower than the Redfield ratio (16) in surface waters (100 m depth).

3.3 Distribution of DON, DOP, and DON/DOP ratio

Studying the DON distribution within a depth of 100 m revealed that the DON concentration ranged from 3.89 to 7.85 μM ($5.62 \pm 1.04 \mu\text{M}$) in typical KW, from 4.96 to 9.09 μM ($6.44 \pm 1.08 \mu\text{M}$) in KW-SCS, from 4.12 to 8.82 μM ($6.19 \pm 1.19 \mu\text{M}$) in KW-ECS, and from 4.10 to 11.2 μM ($7.62 \pm 1.72 \mu\text{M}$) in KW-SCS-RP (Table 4; Figure 3B). The concentration was generally highest in KW-SCS-RP and lowest in KW. Examining the vertical distribution of the DON concentration indicated that; below the nitracline depth, the DON concentration generally decreased with depth (Figure 4). The DOP concentration within a depth of 100 m ranged from 0.15 to 0.29 μM ($0.19 \pm 0.03 \mu\text{M}$) in typical KW, from 0.17 to 0.30 μM ($0.20 \pm 0.04 \mu\text{M}$) in KW-SCS, from 0.13 to 0.29 μM ($0.20 \pm 0.06 \mu\text{M}$) in KW-ECS, and from 0.20 to 0.29 μM ($0.22 \pm 0.06 \mu\text{M}$) in KW-SCS-RP (Table 4; Figure 3B). The concentration thus exhibited negligible variations between the water types, although it was slightly higher in KW-SCS-RP than in KW. The vertical DOP distribution (Figure 6) was noted to be similar to the vertical DON distribution (Figure 4).

The DON/DOP ratio ranged from 16.9 to 51.4 (30.0 ± 7.6) in typical KW, from 29.0 to 47.9 (32.6 ± 6.9) in KW-SCS, from 15.0 to 56.2 (33.2 ± 11.1) in KW-ECS, and from 21.7 to 53.0 (38.6 ± 15.8) in KW-SCS-RP (Table 4). The DON/DOP ratio was highest in KW-SCS-RP and lowest in KW. Overall, the ratio increased with depth for all four water types. The averaged DON/DOP ratio was observed to be considerably higher than the Redfield ratio (16) in all waters.

3.4 Nitrate anomaly

The N^* values within the top 100 m of the water column ranged from 2.04 to 2.65 (2.47 ± 0.16) μM in typical KW (Figure 7), from to

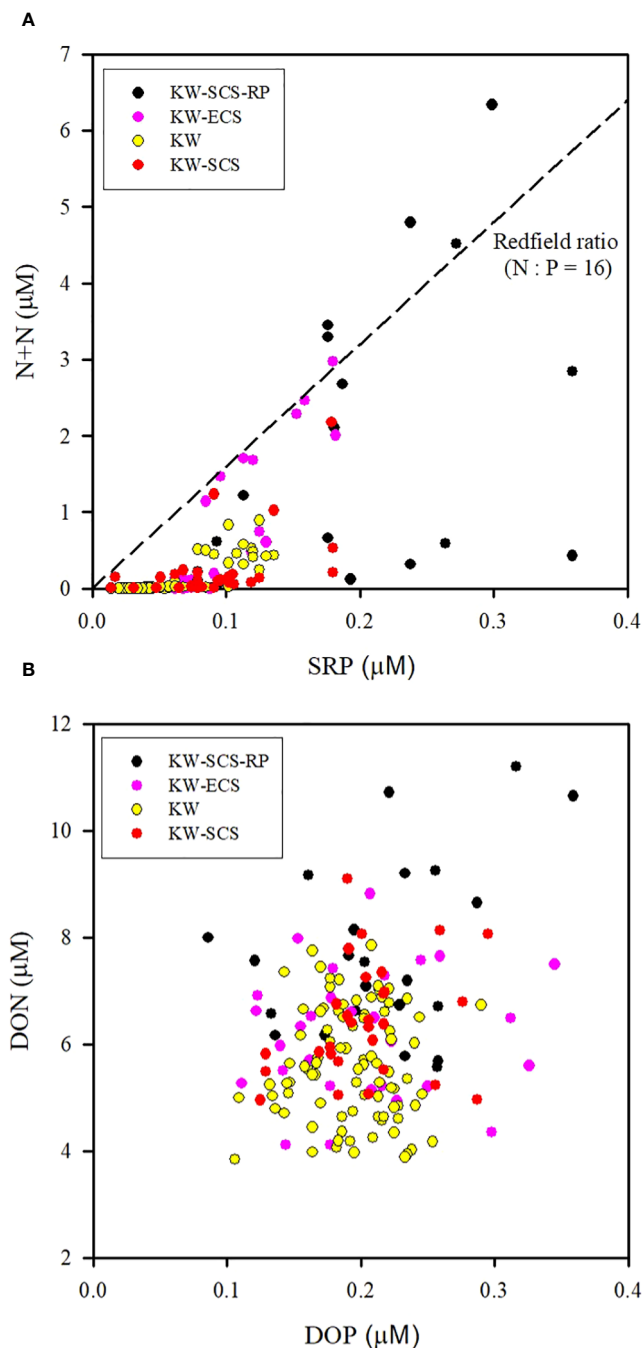


FIGURE 3

Distributions of **(A)** N+N and SRP and **(B)** DON and DOP at the surface above the nutricline depth (100 m) for four water types. Correlations are significant ($p < 0.01$) between N+N and SRP for an individual water type, but correlations are not significant between DON and DOP ($p > 0.05$) for any water type.

1.50 to 2.19 (1.92 ± 0.31) μM in KW-ECS, from 1.26 to 2.69 (1.85 ± 0.52) μM in KW-SCS, and from -0.59 to 2.20 (1.35 ± 1.30) μM in KW-SCS-RP (data omitted for brevity). Overall, N^* decreased with an increase of water depth from the surface to the depth of 100 m (Figure 7). In general, N^* was higher in KW than in the other water types.

3.5 Stratification index

The stratification index (SI) ranged from 2.16 to 3.81 (2.66 ± 0.46) kg m^{-3} in KW, from 2.36 to 3.95 (3.33 ± 0.62) kg m^{-3} in KW-ECS, from 3.20 to 4.00 (3.60 ± 0.032) kg m^{-3} in KW-SCS, and from 3.21 to 3.81 (3.56 ± 0.28) kg m^{-3} in KW-SCS-RP. KW-SCS had the

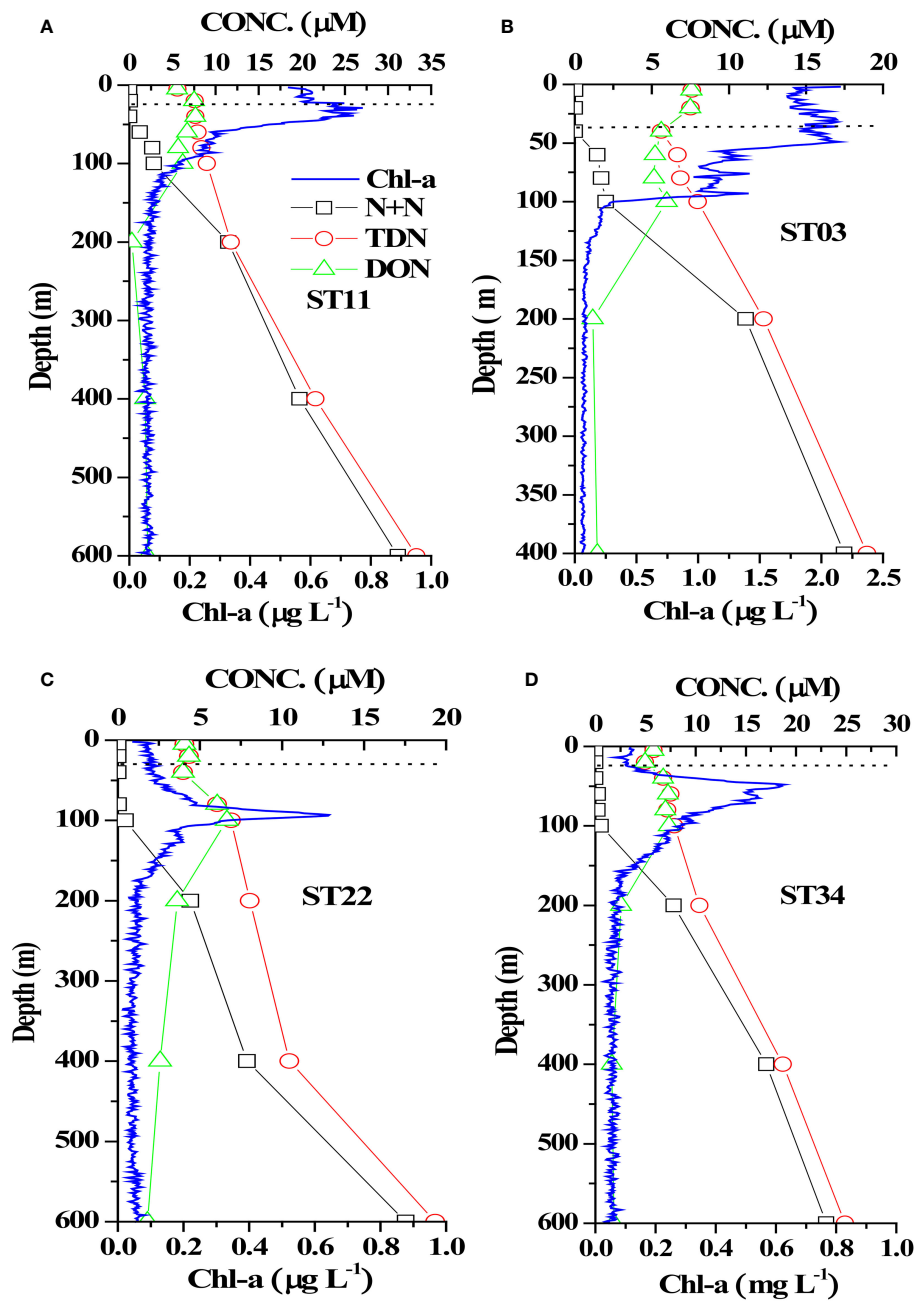


FIGURE 4

Vertical distributions of N+N, TDN, DON, and Chl-a in four stations representing (A) KW-SCS-RP (ST11), (B) KW-ECS (ST03), (C) KW (ST22), and (D) KW-SCS (ST34). The dashed horizontal line indicates the mixed layer depth at each station.

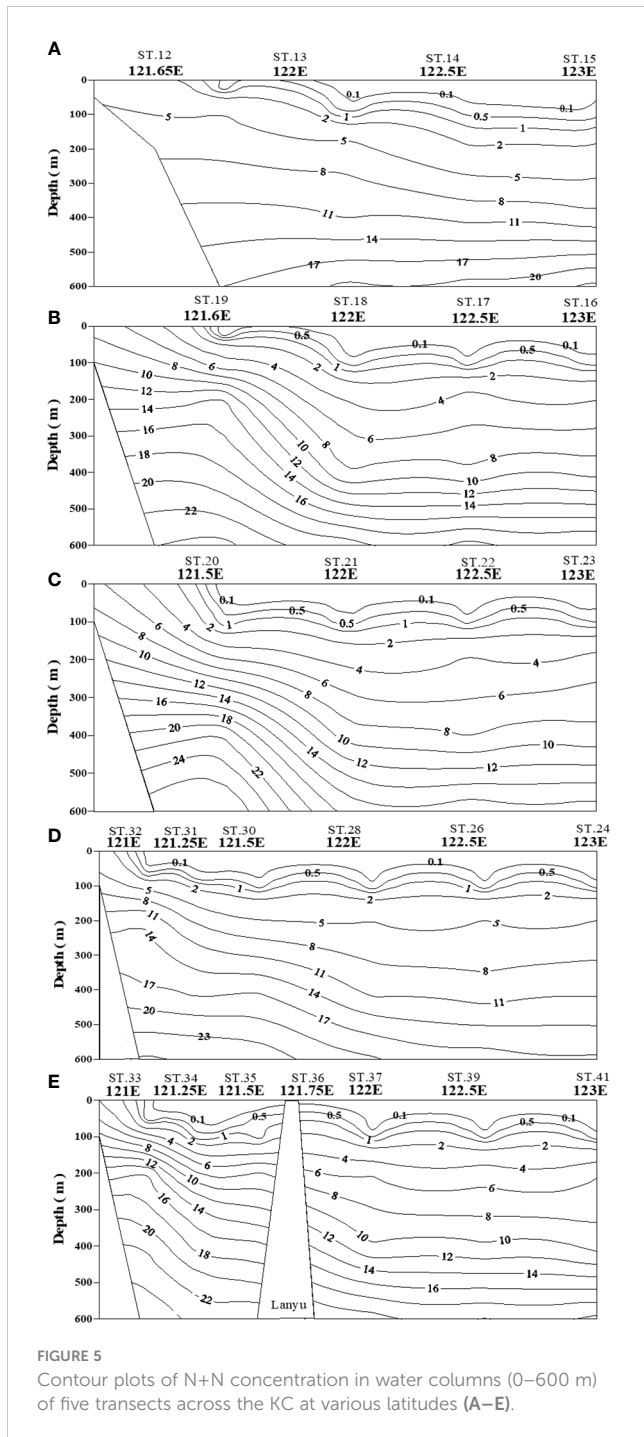
highest SI, followed by KW-SCS-RP, KW-ECS, and KW (data omitted for brevity).

4 Discussion

4.1 Characteristics of water masses and water type classification

At the surface, KW, which originates from the Pacific North Equatorial Current, is characterized by high temperature and

salinity. However, when the KC flows through the region off eastern Taiwan, the properties of the upper KW layers are clearly modified by water exchange processes, particularly exchanges between KW and SCSW and between KW and ECSW; the properties are also modified by coastal uplift of subsurface water and, to a less extent, by the effect of freshwater from small rivers. Consequently, typical surface KW during warm seasons has high surface temperatures (23.63–29.85 °C) and salinity (33.70–34.55) and reaches its highest salinity (34.9) at a depth of 200 m; this is the unique feature of KW, as described elsewhere (Chou et al., 2007; Chen et al., 2017, 2021). The upper water column is highly stratified,



as indicated by the very high SI ($2.18\text{--}3.81\text{ kg m}^{-3}$) in comparison with the criterion for non-stratification ($SI < 0.125\text{ kg m}^{-3}$; De Boyer Montégut et al., 2004). SCSW exhibits lower surface and subsurface temperature and salinity than does in KW at the same depth during warm seasons (Gong et al., 1992; Chen et al., 2014); hence, the surface temperature and salinity are expected to be lower in KW-SCS than in typical KW. However, KW-SCS is also influenced by coastal uplift of subsurface water, particularly in nearshore areas; this condition leads to a decrease in temperature and an increase in salinity in surface and subsurface layers. The SI was determined to range from 3.20 to 3.93 kg m^{-3} in KW-SCS,

indicating the prevailing stratification in the upper 200-m water column. KW-ECS is derived mainly from shelf-edge exchanges and mixing between KW and ECSW and is strongly influenced by upwelling from the KC subsurface layer. Thus, KW-ECS has a lower temperature but higher salinity than does typical KW at the same water depth. The stratification in KW-ECS ($2.37\text{--}4.21\text{ kg m}^{-3}$) was observed to be only slightly higher than that in typical KW ($2.18\text{--}3.81\text{ kg m}^{-3}$). Finally, KW-SCS-RP is mainly affected by coastal uplift of subsurface water and river plumes and has lower temperature and salinity than does typical KW. The SI was also a slightly higher in KW-SCS-RP ($3.14\text{--}3.78\text{ kg m}^{-3}$) than in typical KW due to strong coastal uplift, which lifts up the high-salinity subsurface water. These results thus indicate that water mass exchanges and coastal uplift events are the main determinants of water types and stratification, which in turn affect the distributions of nutrients and biological variables.

4.2 Biophysical controls on vertical and spatial distributions of N+N and SRP

Because the detection limits for N+N and SRP have been established to be as low as 0.7 and 9 nM , respectively, the distribution of N+N and SRP in highly nutrient-depleted surface waters could be reliably assessed. Assessing the vertical distributions of N+N and SRP for all water types revealed that the lowest concentration, which was at the trace level, was observed at the surface. This can be attributed to uptake by phytoplankton and the restriction of a vertical supply of nutrients to the euphotic zone under strong thermal stratification ($SI: 3.05 \pm 0.61\text{ kg m}^{-3}$); it can also be attributed to a much shallower MLD than the nutricline depth in the upper water columns (Figures 4, 6), regardless of upwelling conditions. It is interesting to note that a recent study proposed a long-term decline in the surface nutrient concentrations of the Northwest Pacific Ocean caused by a significant decrease in nutrient inventories of the permanent thermocline (Kim et al., 2022). They also discovered a declining trend in the N:P ratio leading to greater N-limitation. Such findings may have linked to our KC surface waters with considerably low N+N concentration and N-limitation. The N+N and SRP concentrations generally increased with increasing depth below the nutricline depth due to more extensive nutrient regeneration at great depths. Although this study was conducted in spring and summer only, the stratification is likely to be permanent. Chen et al. (2014) reported that the SI values observed for summer and winter were 1.9 ± 0.3 and $1.1 \pm 0.6\text{ kg m}^{-3}$, respectively; these results were obtained from a few measurements sampled from the surface to a depth of 150 m in the upstream region, which was shallower than our method ($0\text{--}200\text{ m}$) in deriving SI values. The N+N and SRP concentrations in surface waters were higher in winter than in summer, likely due to the lower SI in winter (Chen et al., 2014). Accordingly, the thermal stratification is likely persistent and the vertical N+N and SRP distributions are constrained largely by various stratification conditions in four water types throughout the year.

The N+N and SRP concentrations within the upper 100 m of the water column were lowest in typical KW, except for locations influenced by island-induced upwelling (Figure 3A). Such

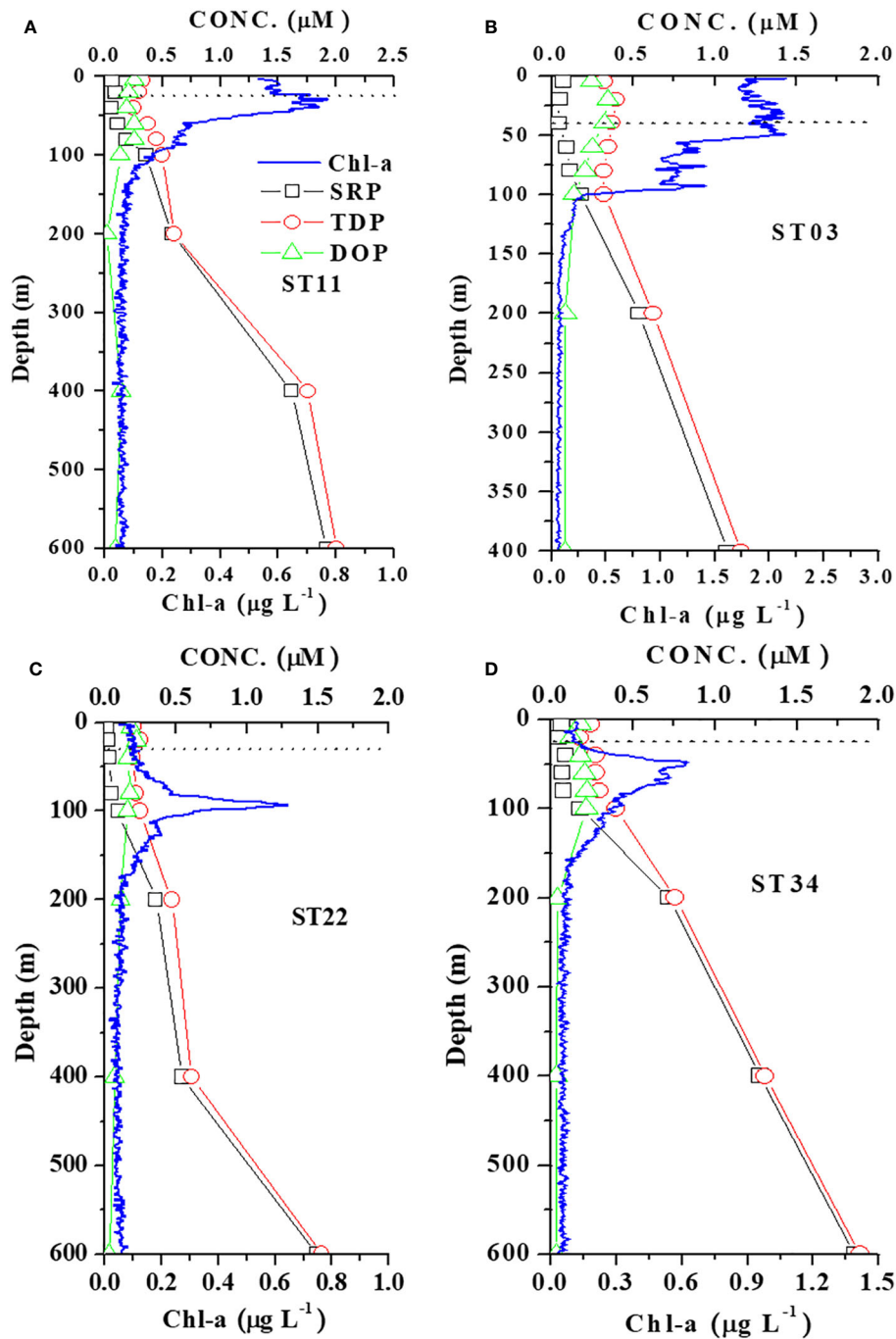


FIGURE 6

Vertical distributions of SRP, TDP, DOP, and Chl-a in four stations representing (A) KW-SCS-RP (ST11), (B) KW-ECS (ST03), (C) KW (ST22), and (D) KW-SCS (ST34). The dashed horizontal line indicates the mixed layer depth at each station.

upwelling generally occurs on the leeward side when the northwardly KC encounters Lanyu Island and Leudao (Green) Island. Hsu et al. (2017) proposed that ocean vortices and island-induced vortex trains were formed on the leeward side of Leudao Island using satellite imagery. The Lanyu-Island-induced upwelling could be clearly observed in the N+N contours of the southernmost transect (ST33–ST41; Figure 5E); an increased N+N concentration was observed around station ST36. The N+N inventory in the top 100 m of the water column increased from 10.78 mmol m⁻² at ST37 to 83.75 mmol

m⁻² at ST36 (a 678% increase), after which it decreased to 12.0 mmol m⁻² for station ST35 (Figure 8B). The SRP inventory also increased from 5.10 mmol m⁻² for station ST 37 to 10.13 mmol m⁻² for station ST36 and then decreased to 5.12 mmol m⁻² for station ST35 (Figure 9B). The N+N and SRP concentrations were high at station ST20, located on the leeward side of Leudao Island; the high concentrations may be due to a combined effect of island-induced upwelling and coastal uplift of subsurface water. The elevated N+N and SRP also resulted in an increase in Chl-a concentration leading to

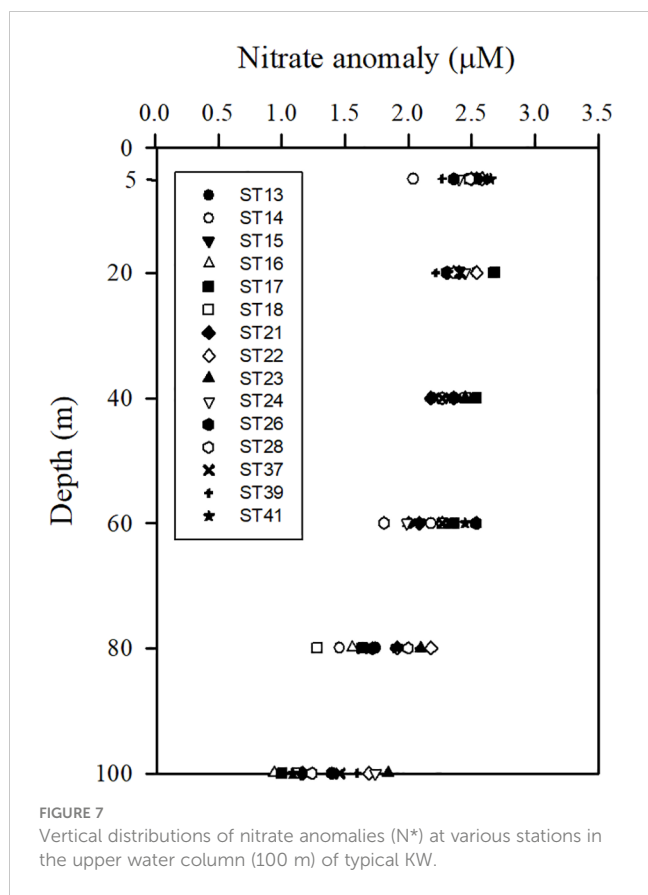


FIGURE 7
Vertical distributions of nitrate anomalies (N*) at various stations in the upper water column (100 m) of typical KW.

a significant correlation between N+N and Chl-*a* ($r = 0.55$, $p < 0.0001$) and between SRP and Chl-*a* ($r = 0.65$, $p < 0.0001$) in typical KW (0–100 m). Island-induced upwelling was also reported previously by Chang et al. (2013), who found that compared with KW, the wake water of the Leudao Island is colder and saltier and has a higher Chl-*a* concentration. Gao et al. (2022) confirmed that the occurrence of phytoplankton bloom in the wakes of islands on the path of the KC accounted for approximately 50% of the increase in surface phytoplankton and that the surface phytoplankton concentration appeared to increase with the size of island located on the KC path and island-induced eddy size.

Coastal uplift of subsurface water may have critical effects on dynamics of nutrients and microbes (Capone and Hutchins, 2013; Davis et al., 2014). The coastal uplift may differ from the coastal upwelling that is largely a wind-induced phenomenon. Nagai et al. (2019) proposed that the turbulent vertical mixing was primarily responsible for the diffusion of subsurface nutrients to the euphotic zone during Kuroshio flowing on the shelf break. The persistent uplifting condition over the coastal zones off eastern Taiwan is primarily related to the transport volume of the KC (Chen et al., 2022), but this process may strongly influence nutrient and phytoplankton conditions in waters other than typical KW. Moreover, studies have reported a persistent and pronounced upwelling on the ECS shelf edge of northeastern Taiwan, which has been demonstrated to carry substantial amounts of cold water and nutrients from the Kuroshio subsurface to the upwelling fields (Liu et al., 2000; Wong et al., 2000). Upwelled nutrients may have substantial effects on nutrient and biological conditions in KW-ECS

and regions downstream of the KC (i.e., beyond Taiwan) (Guo et al., 2012, 2013). Coastal uplifting events increase N+N and SRP concentrations and affect their distributions in KW-SCS, KW-ECS, and KW-SCS-RP. This coastal uplifting or upwelling could be readily observed from temperature, salinity, and N+N contours in various transects across the KC at various latitudes; and is particularly revealed by those stations closest to Taiwan, which—compared with neighboring stations—were noted to be characterized by lower temperatures, higher salinity levels, and higher N+N concentrations (Figure 5; Supplementary Figure 5). Uplifted and upwelled waters were observed to generally originate from deeper layers with lower temperatures, higher salinity levels, and higher N+N and SRP concentrations as well as more abundant phytoplankton. The N+N inventory (above 100-m depth) increased from 14.76 mmol m⁻² at station ST34 to 122.2 mmol m⁻² at station ST33, representing a 728% increase (Figure 8B). Elevated N+N inventory was also observed at coastal station ST19 in the upper north transect (ST16–ST19) (Figure 8A). Similarly, the SRP inventory increased from 8.21 (ST34) to 13.84 (ST33) mmol m⁻², representing a 68.6% increase (Figure 9B), and also increased considerably from ST18 to ST19 in the upper transect (Figure 9A). According to these findings, coastal uplifting may be more intense in summer than spring due to the prevailing southwesterly monsoon in summer. In the data obtained from the summer cruise (OR3–1234), the N+N inventory increased from 6.06 mmol m⁻² at station T2 to 182 mmol m⁻² at station T1 (Figure 8B), and the SRP inventory increased from 6.23 mmol m⁻² at station T2 to 13.1 mmol m⁻² at station T1 (Figure 9B). However, data obtained from the spring cruise (OR3–1217) show less increased concentration than those derived from summer cruises; the N+N inventory increased from 12.3 mmol m⁻² at station K2 to 67.3 mmol m⁻² at station K1 (Figure 8B), and the SRP inventory increased from 3.64 mmol m⁻² at station K2 to 8.7 mmol m⁻² at station T1 (Figure 9B).

Because the N+N and SRP concentrations are mainly determined by biological uptake and uplifting-upwelling supply, the distributions of N+N and SRP in the surface waters (100 m) were strongly correlated ($p < 0.01$) for all water types (Figure 3A); nevertheless, the corresponding slope (b ; $[N+N] = a + b[SRP]$) was lower in typical KW (4.88) and KW-SCS (5.78) than in KW-ECS (19.1) or KW-SCS-RP (11.1). This suggests that coastal uplifting or upwelling can carry water with a higher N/P-ratio to the surface. The pair correlation between Chl-*a* and N+N and that between Chl-*a* and SRP ($r \geq 0.55$, $p < 0.0001$) were highly significant in typical KW, which not only reflects the N+N limitation effect but also indicates positive influence of island-induced upwelling on the N+N, SRP, and Chl-*a* concentrations. However, the pair correlations were nonsignificant for the other water types. This is possibly because coastal uplifting increases the concentrations of nutrients and Chl-*a* separately in surface waters and changes the original patterns of low inorganic nutrient and Chl-*a* concentrations at the surface and high inorganic nutrient and Chl-*a* concentrations in the DCM layer. Nevertheless, the concentration of Chl-*a* in surface waters of coastal zones can be elevated to be as high as 1.2 µg l⁻¹ which was apparently caused by the addition of nutrients. Typical KW had the deepest DCM and greatest nitracline depth of all water types, despite an overall strong correlation between the DCM and nitracline depth (Figure 10A). Meanwhile, the N+N inventory (100 m) correlated inversely with nitracline depth ($r = -0.75$, $p < 0.001$; Figure 10B)

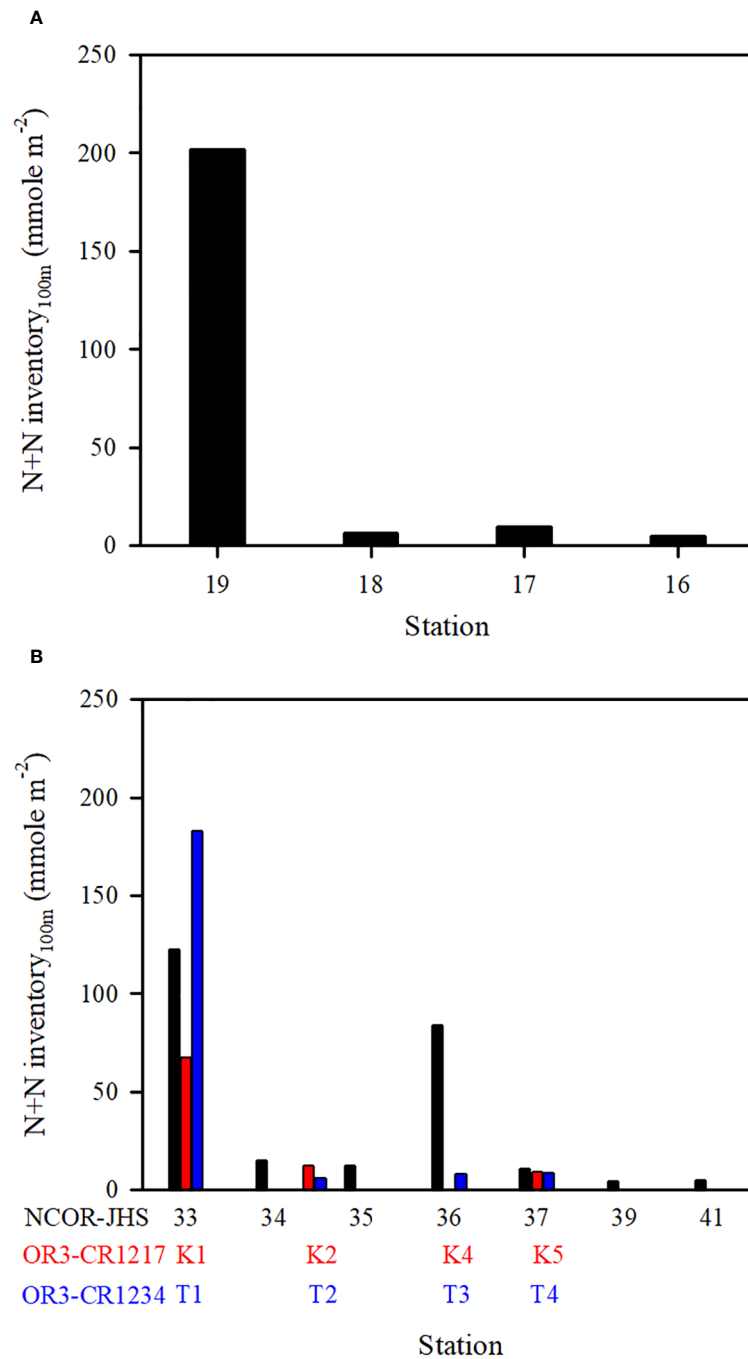


FIGURE 8
 N+N inventory (100 m) at various stations on the transect of (A) stations ST16–ST19 (see N+N contours in Figure 6B; NCOR-JHS Cruise) and (B) stations ST33–ST41 (see N+N contours in Figure 6E; NCOR-JHS Cruise) including the N+N inventory of comparable stations sampled from the OR3-CR1217 (spring) and OR3-CR1234 (summer) cruises.

suggesting that the nitracline depth can be regarded as a proxy of vertical nutrient supply to the euphotic zone (Cermeño et al., 2008) and thus determines the nutrient concentration and inventory in the euphotic zone. In addition, coastal uplifting may result in stronger microbial production and zooplankton grazing in water types other than typical KW (Lai et al., 2021; Chen et al., 2022).

Although coastal uplifting is persistent, the strength was discovered to vary between spring and summer; the mean N+N

and SRP concentrations and inventories shown in the transect across the Kuroshio path are notable difference among spring (April/2007, ORIII-CR1217 Cruise), early summer (May/2006, NCOR-JHS Cruise) and summer (July/2007, ORIII-CR1234 Cruise) (Figures 8B, 9B). The coastal uplifting appears to be stronger in summer than in spring leading to a higher N+N inventory in summer than in spring at the station closest to Taiwan.

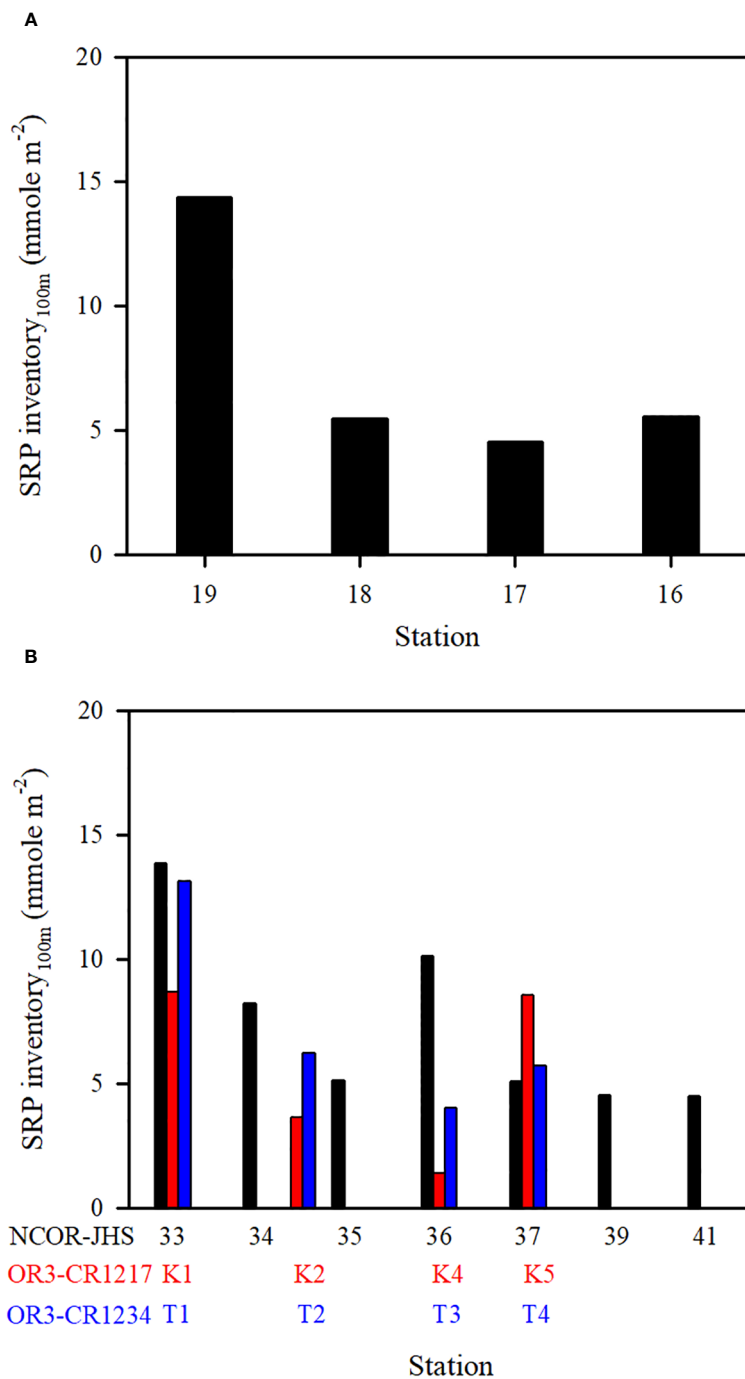


FIGURE 9 SRP inventory (100 m) at various stations on the transect of (A) stations ST16–ST19 (NCOR-JHS Cruise) and (B) stations ST33–ST41 (NCOR-JHS Cruise) including the SRP inventory of comparable stations sampled from the OR3-CR1217 (spring) and OR3-CR1234 (summer) cruises.

4.3 Biophysical controls on the distributions of DON and DOP

In contrast to the results obtained for N+N and SRP, the results obtained from assessing the vertical distributions of DON and DOP indicating that the DON and DOP concentrations were higher at the surface and lower in deep layers, implying clear accumulation of DON and DOP in surface waters and greater degradation at greater

depths for all water types (Figures 4, 6). Surface DON and DOP were likely labile and most of them degraded significantly within the depth range of 100–300 m (Abell et al., 2000; Sipler and Bronk, 2015). The DON and DOP ratio also increased with depth, suggesting faster recycling of DOP than DON. For all water types, DON was more abundant than DOP in surface waters with a considerably higher N/P ratios than the Redfield ratio (16), suggesting the planktonic release of N-rich dissolved organic

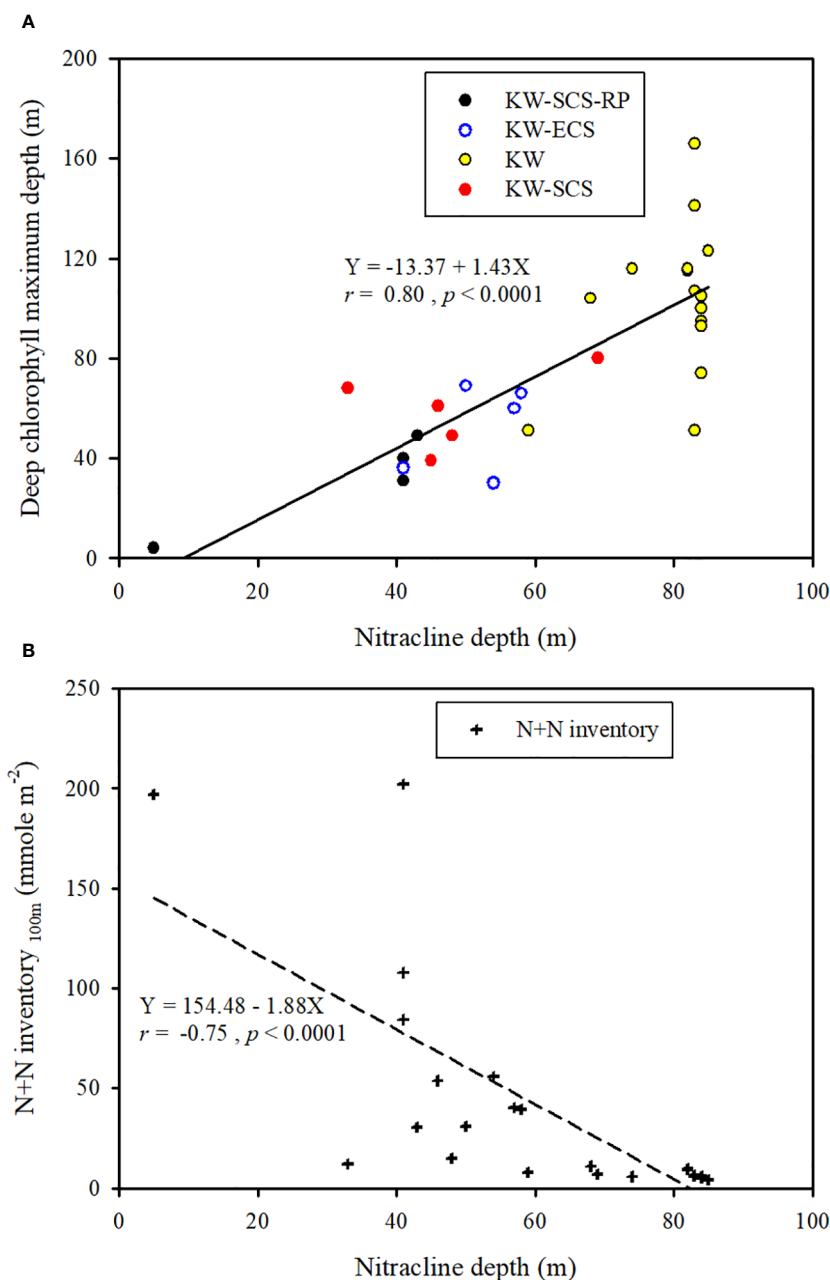


FIGURE 10

Ranges of nitracline depth and chlorophyll maximum depth and overall correlation between nitracline depth and chlorophyll maximum depth (A) and the correlation between nitracline depth and N+N inventory (B) in four water types.

matter into surface waters; such matter may have originated from phytoplankton including N_2 fixers. This also led to a poor correlation ($p > 0.1$) between DON and DOP for all water types.

Hence, this study observed; that the concentration and inventory within the top 100 m of the water column were higher in the water types influenced by coastal uplifting than in typical KW; this is because DON and DOP accumulating near the surface mainly have biological origins. Consequently, the mean DON and DOP concentrations varies between the water types. Specifically, the water types can be ordered (in ascending order) as follows in terms of the mean DON and DOP concentrations: typical KW (DON:

5.62 μM ; DOP: 0.19 μM), KW-ECS (DON: 6.19 μM ; DOP: 0.20 μM), KW-SCS (DON: 6.44 μM ; DOP: 0.21 μM), and KW-SCS-RP (DON: 7.62 μM ; DOP: 0.22 μM). The same trend was observed for the inventory obtained in the top 100 m of the water column: typical KW (DON: 575 mmol m^{-2} ; DOP: 19.3 mmol m^{-2}), KW-ECS (DON: 617 mmol m^{-2} ; DOP: 20.2 mmol m^{-2}), KW-SCS (DON: 621 mmol m^{-2} ; DOP: 19.5 mmol m^{-2}), and KW-SCS-RP (DON: 780 mmol m^{-2} ; DOP: 21.8 mmol m^{-2}). Consequently, significant positive correlations were observed between Chl-*a* and DON in typical KW ($r = 0.47, p < 0.0001$), KW-ECS ($r = 0.41, p < 0.01$), KW-SCS ($r = 0.38, p < 0.005$), and KW-SCS-RP ($r = 0.40, p < 0.01$).

Moreover, positive correlations were observed between Chl-*a* and DOP in typical KW ($r = 0.32$, $p = 0.05$), KW-ECS ($r = 0.45$, $p = 0.005$), KW-SCS ($r = 0.41$, $p = 0.007$), and KW-SCS-RP ($r = 0.46$, $p = 0.005$). The accumulation of DON and DOP in the upper layer may have been primarily due to upwelling-induced biological production and release rather than being due to the physical dilution of upwelled water originally with lower subsurface DON and DOP concentrations (Hung et al., 2003, 2021).

4.4 Constraining N₂ fixation

Recent reports have shown that N₂ fixation is widespread and provides a vital source of new nitrogen in tropical and subtropical oceans where primary production is often limited by N+N (Hansell et al., 2004; Bergman et al., 2013; Shiozaki et al., 2015; Chen et al., 2019; Tang et al., 2019; Wen et al., 2022; Dai et al., 2023). The growth of N₂-fixers is dependent on various factors, among which temperature and nutrient (including iron) availability are regarded as the most critical (Capone and Carpenter, 1982; Mills et al., 2004; Mulholland and Bernhardt, 2005; Sohm et al., 2011; Zehr and Capone, 2020; Wen et al., 2022). The sea surface temperature in our study area typically ranges from 23.63 to 29.85°C in spring and summer; previous studies conducted in some KC areas have reported this temperature to range from 26.4 ± 0.4 to 28.1 ± 0.4°C (Chen et al., 2014) or 26.1 ± 0.2–30.2 ± 0.8°C (Chen et al., 2022). Temperature thus does not appear to be a constraint on N₂ fixation throughout the year, considering that the optimal reported temperature for the growth of *Trichodesmium* is 24–30°C (Breitbart et al., 2007). Nutrients, particularly N+N, were noted to be highly depleted in most surface waters, which were likely to be the critical factor constraining N₂ fixation. Moreover, in this study, the N+N/SRP ratio was observed to be considerably lower than the Redfield ratio (16), implying a strong N- limitation that is critical for N₂ fixation in surface waters.

N₂ fixation was observed to be high, as indicated by the high value of N* in the surface layer of typical KW; this is because in typical KW, the shallow MLD and high SI are favorable for N₂ fixation. Deutsch et al. (2001) proposed that N* values exceeding 2 μM should be considered to indicate great potential for N₂ fixation. At the ALOHA station, N₂ fixation was discovered to be elevated during a period of prolonged stratification (Karl et al., 1997). In addition, Chen et al. (2018) reported considerable abundance of *Trichodesmium* in the downstream area of the KC due to a deep thermocline and a low nitrate concentration in the surface layer. Chen et al. (2014) measured the N₂ fixation rates in an upstream area of the KC, which overlapped with this study's area, and discovered higher rates in warm seasons (180.5 ± 34.3 μmol N m⁻² d⁻¹) than in winter (57.6 ± 29.2 μmol N m⁻² d⁻¹); this was attributed to higher temperature, greater stratification, and lower nutrient concentration in warm seasons. Furthermore, the abundance of *Trichodesmium* and *Crocospaera* in the upstream area of the KC is consistent with the N₂ fixation rate. Despite measurements being conducted in different years, the high rate of N₂ fixation reported by Chen et al. (2014) is in good agreement with our high N* values observed in typical KW in warm seasons. Most of these high N* values were observed in the

surface (0–60 m) of KW (Figure 7); these values are consistent with previously reported N₂ fixation rates (67±12%) occurred mainly in shallow depths (0–45 m) and the fixation rate decreased from the surface to a depth of 125 m at the ALOHA station (Böttjer et al., 2017). Additionally, the concentration of N* was inversely correlated with the concentration of N+N ($r = -0.76$, $p < 0.01$) and the N+N/SRP ratio ($r = -0.71$, $p < 0.01$) in the surface layer of typical KW. However, these correlations were nonsignificant in the surface layer for the other water types, and this is due to the strong influence of coastal uplifting. N* was also inversely correlated with SRP level ($r = -0.98$, $p < 0.001$) in typical KW, and this can be attributed to the substantial requirement of SRP by N₂ fixers during N₂ fixation. N₂ fixation thus appears to play a crucial role in shaping nutrient and biological conditions and dynamics in surface KW. N₂ fixation was overall less extensive in other water types regarding higher N* values in typical KW (2.47 ± 0.16 μM) than those in KW-ECS (1.92 ± 0.31 μM), KW-SCS (1.85 ± 0.52 μM), and KW-SCS-RP (1.35 ± 1.30 μM), resulted likely from the impacts of coastal nutrient injection into sunlit layers in waters other than typical KW.

In the study area, nitrogen fixation may be promoted by Fe availability in warm seasons, although Fe has generally hypothesized to limit N₂ fixation in the tropical North Pacific (Brown et al., 2005; Grabowski et al., 2008). Scholars have demonstrated that the northeast monsoon carries a substantial amount of Fe-rich eolian dust from the Gobi Desert to the Northwestern Pacific and associated marginal seas (Duce et al., 1991; Wu et al., 2003; Wang et al., 2011; Wang and Ho, 2020; Kurisu et al., 2021). König et al. (2022) also reported that dust-derived Fe deposition in the North Pacific was highest in spring and early summer. Wang and Ho (2020) indicated that the Fe deposition rate and dissolved Fe concentration was higher in spring than in summer in an area close to our study area. Several studies have linked Asian dust deposition to increase in Chl-*a* and dissolved Fe concentrations in the SCS, which are associated with the bloom of N₂ fixers (Wu et al., 2003; Wong et al., 2007; Wang et al., 2011; Dai et al., 2023). These authors further indicated that the onset of nitrogen fixation is in phase with the atmospheric deposition of land-derived dust in the northern SCS. Although data on dissolved Fe are limited, Sato et al. (2021) examined the distribution of dissolved Fe along the KC and observed that the concentration in the mixed layer was higher at three stations off eastern Taiwan (0.190–0.280 nM) than in most stations across the Okinawa Trough (0.159–0.360 nM) and stations off Tosa Bay in Japan (0.170–0.204 nM). The concentration range in the KC off eastern Taiwan is close to the range observed by Wang and Ho (2020) for nearby stations (0.28–0.74 nM), providing evidence of a high load of Asian dust in the upstream areas of the KC. Therefore, dissolved Fe is likely favorable for N₂ fixation in warm seasons in the upstream areas of the KC.

4.5 Implications of upwelling and N₂ fixation in the oligotrophic KC

Despite considerable oligotrophy, many fish species use the KC region as spawning and nursery grounds (Chiu and Huang, 1994; Chen et al., 2022), and this renders the KC region a favorable fishing ground. Specifically, oligotrophic KW regions with low Chl-*a*

concentrations and primary productivity are often dominated by small phytoplankton, but known as high fishery production regions, yielding the “Kuroshio Paradox” (Nagai et al., 2019; Saito, 2019, 2021; Chen et al., 2022). The efficiency of energy transfer from primary production to higher trophic levels is generally low in an oligotrophic system, creating the Kuroshio Paradox. Saito (2019) explained this phenomenon as being caused by the coastal injection of nutrients to the euphotic zone that promotes new primary production and rapid energy transfer from primary producers to higher trophic levels in warm waters. The arguments are based mainly on the findings in downstream KC regions associated with the interaction of the KC and the continental shelf. On the basis of observations from a transect across the path of the KC off northeastern Taiwan, Chen et al. (2022) concluded that persistent coastal uplift of subsurface water increased the abundance of surface nutrients and Chl-*a* concentrations and changed the phytoplankton community to support more energy being transferred to higher trophic levels. Nagai et al. (2019); Nagai et al. (2021), however, regarded the influence of both coastal injection and seamounts on nutrient supply to sunlit layers as being crucial mechanisms to the relief of oligotrophic conditions and an explanation for the Kuroshio Paradox.

Herein, we propose multi-faceted processes that enhance nutrient availability, primary production, and efficiency of energy transfer from primary producers to higher trophic levels in warm and oligotrophic KC. First, coastal uplift of subsurface water increases nutrient availability and the amount of biomass (Chl-*a*) in the coastal zones of the study area, leading to major increases in primary production in all water types, except for typical KW. Second, island-induced upwelling causes increases in inorganic nutrients and Chl-*a* in the wake waters of small islands located in typical KW. Third, nitrogen fixation occurs widely in all water types and is most extensive in typical KW. N₂ fixation may occur in all seasons, and this is supported by the findings of the present and previous studies; this fixation may be a vital food source for the oligotrophic food web. Finally, in KW, the high surface abundance of DON and DOP, as identified in the present study, and high surface abundance of DOC (75–82 μM), as discovered previously (Hung et al., 2000, 2003; Wu et al., 2015), may increase the likelihood of a microbial loop in which carbon and energy are transferred to higher trophic levels through bacteria’s utilization of dissolved organic matter. The microbial loop has been widely reported to serve alongside primary production as a carbon source for the food web, particularly in oligotrophic oceans (Azam et al., 1983; Williams and Ducklow, 2019; Glibert and Mitra, 2022). Lai et al. (2021) also demonstrated the crucial role of bacteria in the cycling of organic carbon and nutrients and in the transfer of trophic energy in SCS-KC mixing zones. Accordingly, numerous physical and biogeochemical processes may be responsible for the oligotrophic KC serving as good fishery grounds and may thus explain the scenario Kuroshio Paradox.

5 Conclusion

Reliable analytical methods for determining the levels of inorganic and organic nutrients are essential for designing physical and biogeochemical controls on the distributions and

dynamics of inorganic and organic nutrients in oligotrophic KC. This study determined four types of water derived from KC through various mixing, exchange, and upwelling processes. Typical KW was observed to be highly oligotrophic and to have ultralow concentrations of N+N and SRP but high concentrations of DON and DOP above the nutricline depth, which could primarily be attributed to strong and permanent surface stratification. However, the nutrient and Chl-*a* conditions of typical KW were modified locally by island-induced upwelling. In water types other than typical KW, the concentrations of inorganic and organic nutrients were elevated to varying degrees owing to the mixing of water masses and coastal uplifting processes. Moreover, various degrees of N+N limitation and high N* values were observed near the surface, confirming the occurrence of extensive N₂ fixation in typical KW and less extensive N₂ fixation in other water types. N₂ fixation could also contribute to a considerably high DON/DOP ratio at the surface of typical KW. N₂ fixation, various upwelling activities, and possibly an enhanced microbial loop supported by enriched organic nutrients may explain the Kuroshio paradox in the oligotrophic KC. Overall, the aforementioned physical and biogeochemical processes determine the upper-ocean distributions of N+N, SRP, DON, DOP, and Chl-*a* in the KC area off eastern Taiwan in warm seasons.

Data availability statement

The original contributions presented in the study are included in the article/Supplementary Material. Further inquiries can be directed to the corresponding author.

Author contributions

JH: Conceptualization, Data curation, Funding acquisition, Investigation, Project administration, Resources, Writing – original draft, Writing – review & editing. ST: Data curation, Formal analysis, Investigation, Writing – original draft. YL: Data curation, Formal analysis, Writing – original draft. ZH: Investigation, Writing – original draft.

Funding

The author(s) declare financial support was received for the research, authorship, and/or publication of this article. This study was supported by the National Science Council and Ministry of Science and Technology, Taiwan, Republic of China (NSC 100-2621-M110-002, MOST 106-2611-M-110-015-, MOST 110-2611-M-110-011-, and NSTC 112-2611-M-110-001-).

Acknowledgments

The authors would like to sincerely thank Dr. Yi Yang for leading the NCOR-JHS cruise and arranging sample collection

during the cruise. We also thank Mrs. Y-T Yeh and M-H Huang for their assistance in sampling and analyses.

Conflict of interest

Author S-HT was employed by the company SGS Taiwan Ltd.

The remaining authors declare that the research was conducted in the absence of any commercial or financial relationships that could be construed as a potential conflict of interest.

The author(s) declared that they were an editorial board member of Frontiers, at the time of submission. This had no impact on the peer review process and the final decision.

References

- Abell, J., Emerson, S., and Renaud, P. (2000). Distributions of TOP, TON and TOC in the North Pacific subtropical gyre: Implications for nutrient supply in the surface ocean and remineralization in the upper thermocline. *J. Mar. Res.* 58, 203–222. doi: 10.1357/002224000321511142
- Azam, T., Field, J. G., Gray, J. S., Reil, M. L. A., and Thingstad, F. (1983). The ecological role of water-column microbes in the sea. *Mar. Ecol. Prog. Ser.* 10, 257–263. doi: 10.3354/meps010257
- Bergman, B., Sandh, G., Lin, S., Larsson, J., and Carpenter, E. J. (2013). *Trichodesmium*—a widespread marine cyanobacterium with unusual nitrogen fixation properties. *FEMS Microbiol. Rev.* 37, 286302. doi: 10.1111/j.1574-6976.2012.00352.x
- Berman, T., and Bronk, D. A. (2003). Dissolved organic nitrogen: A dynamic participant in aquatic ecosystems. *Aquat. Microb. Ecol.* 31, 279–305. doi: 10.3354/ame031279
- Böttjer, D., Dore, J. E., Karl, D. M., Letelier, R. M., Mahaffey, C., Wilson, S., et al. (2017). Temporal variability of nitrogen fixation and particulate nitrogen export at Station ALOHA. *Limnol. Oceanogr.* 62. doi: 10.1002/lno.10386
- Braman, R. S., and Hendrix, S. A. (1989). Nanogram nitrite and nitrate determination in environmental and biological materials by vanadium (III) reduction with chemiluminescence detection. *Anal. Chem.* 61, 27162718. doi: 10.1021/ac00199a007
- Breitbarth, E., Oschlies, A., and LaRoche, J. (2007). Physiological constraints on global distribution of *Trichodesmium*—effect of temperature on diazotrophy. *Biogeochemistry* 4, 5361. doi: 10.5194/bg-4-53-2007
- Bronk, D. A., and Ward, B. B. (2000). Magnitude of DON release relative to gross nitrogen uptake in marine systems. *Limnol. Oceanogr.* 45, 18791883. doi: 10.4319/lo.2000.45.8.1879
- Brown, M. T., Landing, W. M., and Measures, C. I. (2005). Dissolved and particulate Fe in the western and central North Pacific: Results from the 2002 IOC cruise. *Geochim. Geophys. Geosyst.* 6, Q10001. doi: 10.1029/2004GC000893
- Browning, T. J., and Moore, C. M. (2023). Global analysis of ocean phytoplankton nutrient limitation reveals high prevalence of co-limitation. *Nat. Commun.* 14. doi: 10.1038/s41467-023-40774-0
- Capone, D. G., and Carpenter, E. J. (1982). Nitrogen fixation in the marine environment. *Science*. 217, 1140–1142. doi: 10.1126/science.217.4565.1140
- Capone, D. G., and Hutchins, D. A. (2013). Microbial biogeochemistry of coastal upwelling regimes in a changing ocean. *Nat. Geosci.* 6, 711717. doi: 10.1038/ngeo1916
- Capone, D. G., Zehr, J., Paerl, H., Bergman, B., and Carpenter, E. (1997). *Trichodesmium*, a globally significant marine cyanobacterium. *Science*. 276, 1221–1229. doi: 10.1126/science.276.5316.1221
- Cermeño, P., Dutkiewicz, S., Harris, R. P., Follows, M., Schofield, O., and Falkowski, P. G. (2008). The role of nitricine depth in regulating the ocean carbon cycle. *Proc. Nat. Acad. Sci.* 105. doi: 10.1073/pnas.0811302106
- Chang, M.-H., Tang, T.-Y., Ho, C.-R., and Chao, S.-Y. (2013). Kuroshio-induced wake in the lee of Green Island off Taiwan. *J. Geophys. Res.: Oceans* 118, 15081519. doi: 10.1002/jgrc.20151
- Chen, L.-L., Chen, H.-Y., Lin, Y.-H., Yong, T.-C., Taniuchi, Y., and Tuo, S.-h. (2014). The relative contributions of unicellular and filamentous diazotrophs to N₂ fixation in the South China Sea and the upstream Kuroshio. *Deep-Sea Res.* 185, 5671. doi: 10.1016/j.dsr.2013.11.006
- Chen, C.-T. A., Huang, T.-H., Wu, C.-H., Yang, H., and Guo, X. (2021). Variability of nutrient stream near Kuroshio's origin. *Sci. Rep.* 11, 5080. doi: 10.1038/s41598-021-84420-5
- Chen, C.-C., Jan, S., Kuo, T.-H., and Li, S.-Y. (2017). Nutrient flux and transport by the Kuroshio east of Taiwan. *J. Mar. Syst.* 167, 43–54. doi: 10.1016/j.jmarsys.2016.11.004
- Chen, C.-C., Lu, C.-Y., Jan, S., C.-h., H., and Chung, C.-C. (2022). Effects of the coastal uplift on the Kuroshio ecosystem, eastern Taiwan, the Western Boundary Current of the North Pacific Ocean. *Front. Mar. Sci.* 9. doi: 10.3389/fmars.2022.796187
- Chen, M., Lu, Y., Jiao, N., Tian, J., Kao, S.-J., and Zhang, Y. (2019). Biogeographic drivers of diazotrophs in the western Pacific Ocean. *Limnol. Oceanogr.* 64, 14031421. doi: 10.1002/lno.11123
- Chen, Y. Y., Sun, X. X., and Zhu, M. L. (2018). Net-phytoplankton communities in the Western Boundary Currents and their environmental correlations. *Chin. J. Oceanol. Limnol.* 30. doi: 10.1007/s00343-017-6261-8
- Chen, C.-T. A., and Wang, S.-L. (1998). Influence of intermediate water in the western Okinawa Trough by the outflow from the South China Sea. *J. Geophys. Res.* 103, 12683–12688. doi: 10.1029/98JC00366
- Chiu, T.-S., and Huang, J.-B. (1994). Kuroshio and its related fishes of Taiwan: Review and prospective inferred from ichthyoplankton. *J. Fish. Soc. Taiwan* 21, 157168.
- Chou, W. C., Sheu, D. D., Chen, C. T. A., Wen, L. S., Yang, Y., and Wei, C. L. (2007). Transport of the South China Sea subsurface water outflow and its influence on the carbon chemistry of Kuroshio waters off southeastern Taiwan. *J. Geophys. Res.* 112, C12008. doi: 10.1029/2007JC004087
- Dai, M., Luo, Y.-W., Achterberg, E. P., Browning, T. J., Cai, Y., Cao, Z., et al. (2023). Upper ocean biogeochemistry of the oligotrophic North Pacific Subtropical Gyre: From nutrient sources to carbon export. *Rev. Geophys.* 61, e2022RG000800. doi: 10.1029/2022RG000800
- Davis, K. A., Banas, N. S., Giddings, S. N., Siedlecki, S. A., MacCreedy, P., Lessard, E. J., et al. (2014). Estuary-enhanced upwelling of marine nutrients fuels coastal productivity in the U.S. Pacific Northwest. *J. Geophys. Res.: Oceans* 119, 8778–8799. doi: 10.1002/2014JC010248
- De Boyer Montégut, C., Madec, G., Fischer, A. S., Lazar, A., and Ludicone, D. (2004). Mixed layer depth over the global ocean: an examination of profile data and a profile-based climatology. *J. Geophys. Res.* 109, C12003. doi: 10.1029/2004JC002378
- Deutsch, C., Gruber, N., Key, R. M., Sarmiento, J. L., and Ganachaud, A. (2001). Denitrification and N₂ fixation in the Pacific Ocean. *Glob. Biogeochem. Cycles* 15, 483–506. doi: 10.1029/2000GB001291
- Duce, R. A., Liss, P. S., Merrill, J. T., Atlas, E. L., Buat-Menard, P., Hicks, B. B., et al. (1991). The atmospheric input of trace species to the world ocean. *Glob. Biogeochem. Cycles* 5, 193–259. doi: 10.1029/91GB01778
- Dyrhman, S. T., Chappell, P. D., Haley, S. T., Moffett, J. W., Orchard, E. D., Waterbury, J. B., et al. (2006). Phosphonate utilization by the globally important marine diazotroph *Trichodesmium*. *Nature* 439, 6871. doi: 10.1038/nature04203
- Filella, A., Riemann, L., Van Wambeke, F., Pulido-Villena, E., Vogts, A., Bonnet, S., et al. (2022). Contrasting roles of DOP as a source of phosphorus and energy for marine diazotrophs. *Front. Mar. Sci.* 9. doi: 10.3389/fmars.2022.923765
- Gao, J., Guo, X., Yoshie, N., and Ding, X. (2022). Occurrence of surface phytoplankton bloom as the Kuroshio Current passes an island. *J. Geophys. Res.: Oceans* 127, e2021JC018242. doi: 10.1029/2021JC018242

Publisher's note

All claims expressed in this article are solely those of the authors and do not necessarily represent those of their affiliated organizations, or those of the publisher, the editors and the reviewers. Any product that may be evaluated in this article, or claim that may be made by its manufacturer, is not guaranteed or endorsed by the publisher.

Supplementary material

The Supplementary Material for this article can be found online at: <https://www.frontiersin.org/articles/10.3389/fmars.2024.1383244/full#supplementary-material>

- Gao, Y., Wang, L., Guo, X., Xu, Y., and Luo, L. (2020). Atmospheric wet and dry deposition of dissolved inorganic nitrogen to the South China Sea. *Sci. China Earth Sci.* 63. doi: 10.1007/s11430-019-9612-2
- Garside, C. (1982). A chemiluminescent technique for the determination of nanomolar concentrations of nitrate and nitrite in seawater. *Mar. Chem.* 11, 159167. doi: 10.1016/0304-4203(82)90039-1
- Glibert, P. M., and Mitra, A. (2022). From webs, loops, shunts, and pumps to microbial multitasking: Evolving concepts of marine microbial ecology, the mixoplankton paradigm, and implications for a future ocean. *Limnol. Oceanogr.* 67, 585–597. doi: 10.1002/lno.12018
- Gong, G. C., Liu, K. K., Liu, C.-T., and Pai, S.-C. (1992). The chemical hydrography of the South China Sea west of Luzon and a comparison with the west Philippine Sea. *Terrest. Atmo. Ocean. Sci.* 3, 587–602. doi: 10.3319/TAO.1992.3.4.587(O)
- Grabowski, M. N. W., Church, M. J., and Karl, D. M. (2008). Nitrogen fixation rates and 526 controls at Stn ALOHA. *Aquat. Microb. Ecol.* 52, 175–183. doi: 10.3354/ame01209
- K. Grasshoff, M. Ehrhardt and K. Kremling (Eds.) (1983). *Methods of Seawater Analysis* (Weinheim: Verlag Chemie), 419. pp.
- Graziano, L. M., Geider, R. J., Li, W. K. W., and Olaiyola, M. (1996). Nitrogen limitation of North Atlantic phytoplankton: analysis of physiological condition in nutrient enrichment experiments. *Aquat. Microb. Ecol.* 11, 5364. doi: 10.3354/ame011053
- Gruber, N., and Sarmiento, J. L. (1997). Global patterns of marine nitrogen fixation and denitrification. *Glob. Biogeochem. Cycles* 11, 235266. doi: 10.1029/97GB00077
- Guo, X., Zhu, X.-H., Long, Y., and Huang, D. J. (2013). Spatial variations in the Kuroshio nutrient transport from the East China Sea to south of Japan. *Biogeosciences* 10, 6403–6417. doi: 10.5194/bg-10-6403-2013
- Guo, X., Zhu, X.-H., Wu, Q.-S., and Huang, D. (2012). The Kuroshio nutrient stream and its temporal variation in the East China Sea. *J. Geophys. Res.: Oceans* 117, C01026. doi: 10.1029/2011JC007292
- Hansell, D. A., Bates, N. R., and Olson, D. B. (2004). Excess nitrate and nitrogen fixation in the North Atlantic Ocean. *Mar. Chem.* 84, 243265. doi: 10.1016/j.marchem.2003.08.004
- Hansell, D. A., and Feely, R. A. (2000). Atmospheric intertropical convergence impacts surface ocean carbon and nitrogen biogeochemistry in the western tropical Pacific. *Geophys. Res. Lett.* 27, 10131016. doi: 10.1029/1999GL002376
- Hsin, Y.-C., Qiu, B., Chiang, T.-L., and Wu, C.-R. (2013). Seasonal and interannual variations in the intensity and central position of the surface Kuroshio east of Taiwan. *J. Geophys. Res.: Oceans* 118, 43054316. doi: 10.1002/jgrc.20323
- Hsu, P.-C., Chang, M.-H., Lin, C.-C., Huang, S.-J., and Ho, C.-R. (2017). Investigation of the island-induced ocean vortex train of the Kuroshio Current using satellite imagery. *Remot. Sens. Environ.* 193. doi: 10.1016/j.rse.2017.02.025
- Hu, D., Wu, L., Cai, W., Gupta, A. S., Ganachaud, A., Qiu, B., et al. (2015). Pacific western boundary currents and their roles in climate. *Nature* 522, 299308. doi: 10.1038/nature14504
- Hung, J.-J., Chen, C.-H., Gong, G.-C., Sheu, D. D., and Shiah, F.-K. (2003). Distributions, stoichiometric patterns and cross-shelf exports of dissolved organic matter in the East China Sea. *Deep-Sea Res. II* 50, 11271145. doi: 10.1016/S0967-0645(03)00014-6
- Hung, J.-J., Hung, C.-S., and Su, H.-M. (2008). Biogeochemical responses to the removal of maricultural structures from the eutrophic Lagoon (Tapong Bay) in Taiwan. *Mar. Environ. Res.* 65, 1–17. doi: 10.1016/j.marenvres.2007.07.003
- Hung, J.-J., Lin, P.-L., and Liu, K.-K. (2000). Dissolved and particulate organic carbon in the southern East China Sea. *Cont. Shelf Res.* 20, 545569. doi: 10.1016/S0278-4343(99)00085-0
- Hung, J.-J., Wang, S.-M., and Chen, Y.-L. (2007). Biogeochemical controls on distributions and fluxes of dissolved and particulate organic carbon in the Northern South China Sea. *Deep-Sea Res. II* 54, 1486–1503. doi: 10.1016/j.dsr2.2007.05.006
- Hung, J.-J., Wang, Y.-H., Fu, K.-H., Lee, I.-H., Tsai, S.-H., Lee, C.-Y., et al. (2021). Biogeochemical responses to internal-wave impacts in the continental margin off Dongsha Atoll in the northern South China Sea. *Prog. Oceanogr.* 199. doi: 10.1016/j.pcean.2021.102689
- Isada, T., Hattori-Saito, A., Saito, H., Kondo, Y., Nishioka, J., Kuma, K., et al. (2019). Responses of phytoplankton assemblages to iron availability and mixing water masses during the spring bloom in the Oyashio region, NW Pacific. *Limnol. Oceanogr.* 64, 197–216. doi: 10.1002/lno.11031
- Jackson, G. A., and Williams, P. M. (1985). Importance of dissolved organic nitrogen and phosphorus to biological nutrient cycling. *Deep-Sea Res.* 32, 223235. doi: 10.1016/0198-0149(85)90030-5
- Jin, H., Zhang, C., Meng, S., Wang, Q., Ding, X., Meng, L., et al. (2024). Atmospheric deposition and river runoff stimulate the utilization of dissolved organic phosphorus in coastal seas. *Nat. Commun.* 15. doi: 10.1038/s41467-024-44838-7
- Joh, Y., Di Lorenzo, E., Siqueira, L., and Kirtman, B. P. (2021). Enhanced interactions of Kuroshio Extension with tropical Pacific in a changing climate. *Sci. Rep.* 11, 6247. doi: 10.1038/s41598-021-85582-y
- Karl, D. M., and Björkman, K. M. (2015). “Dynamics of dissolved organic phosphorus,” in *Biogeochemistry of Marine Dissolved Organic Matter*. Eds. D. A. Hansell and C. A. Carlson (Academic Press, Burlington), 233334.
- Karl, D., Letelier, R., Tupas, L., Dore, J., Christian, J., and Hebel, D. (1997). The role of nitrogen fixation in biogeochemical cycling in the subtropical North Pacific Ocean. *Nature* 388, 535358. doi: 10.1038/41474
- Karl, D. M., and Tien, G. (1992). Magic: A sensitive and precise method for measuring dissolved phosphorus in aquatic environments. *Limnol. Oceanogr.* 37, 105116. doi: 10.4319/lo.1992.37.1.0105
- Kim, J., Kim, G., Cho, H.-M., Nam, S., Hwang, J., Park, S., et al. (2022). Decline in the nutrient inventories of the upper subtropical Northwest Pacific Ocean. *Geophys. Res. Lett.* 49, 9. doi: 10.1029/2021GL093968
- Kim, I.-N., Lee, K., Gruber, N., Karl, D. M., Bullister, J. L., Yang, S., et al. (2014). Increasing anthropogenic nitrogen in the North Pacific Ocean. *Science* 346, 6213. doi: 10.1126/science.1258396
- Kodama, T., Nishimoto, A., Horii, S., Ito, D., Yamaguchi, T., Hidaka, K., et al. (2021). Spatial and seasonal variations of stable isotope ratios of particulate organic carbon and nitrogen in the surface water of the Kuroshio. *J. Geophys. Res.: Oceans* 126. doi: 10.1029/2021JC017175
- Komatsu, K., and Hiroe, Y. (2019). “Structure and impact of the kuroshio nutrient stream,” in *Kuroshio Current: Physical, Biogeochemical, and Ecosystem Dynamics*. Eds. T. Nagai, H. Saito, K. Suzuki and M. Takahashi (AGU-Wiley, Washington, D.C., USA). doi: 10.1002/9781119428428.ch5
- König, D., Conway, T. M., Hamilton, D. S., and Tagliabue, A. (2022). Surface ocean biogeochemistry regulates the impact of anthropogenic aerosol Fe deposition on the cycling of iron and iron isotopes in the North Pacific. *Geophys. Res. Lett.* 49, e2022GL098016. doi: 10.1029/2022GL098016
- Kurisu, M., Sakata, K., Uematsu, M., Ito, A., and Takahashi, Y. (2021). Contribution of combustion Fe in marine aerosols over the northwestern Pacific estimated by Fe stable isotope ratios. *Atm. Chem. Phys.* 21, 1602716050. doi: 10.5194/acp-21-16027-2021
- Lai, C.-C., Wu, C.-R., Chuang, C.-Y., Lee, K.-Y., Kuo, H.-Y., and Shiah, F.-K. (2021). Phytoplankton and bacterial responses to monsoon-driven water masses mixing in the Kuroshio off the east coast of Taiwan. *Front. Mar. Sci.* 8. doi: 10.3389/fmars.2021.707807
- Liang, Z., Letscher, R., and Knapp, A. N. (2022). Dissolved organic phosphorus concentrations in the surface ocean controlled by both phosphate and iron stress. *Nat. Geosci.* 15. doi: 10.1038/s41561-022-00988-1
- Liu, K.-K., Su, M.-J., Hsueh, C.-R., and Gong, G.-C. (1996). The nitrogen isotopic composition of nitrate in the Kuroshio Water northeast of Taiwan: evidence for nitrogen fixation as a source of isotopically light nitrate. *Mar. Chem.* 54, 273292. doi: 10.1016/0304-4203(96)00034-5
- Liu, K.-K., Tang, T.-Y., Gong, G.-C., Chen, L.-Y., and Shiah, F.-K. (2000). Cross-shelf and along-shelf nutrient fluxes derived from flow fields and chemical hydrography observed in the southern East China Sea off northern Taiwan. *Cont. Shelf Res.* 20, 493523. doi: 10.1016/S0278-4343(99)00083-7
- Lomas, M. W., Burke, A. L., Lomas, D. A., Bell, D. W., Shen, C., Dyhrman, S. T., et al. (2010). Sargasso Sea phosphorus biogeochemistry: an important role for dissolved organic phosphorus (DOP). *Biogeosciences* 7, 695710. doi: 10.5194/bg-7-695-2010
- Lozier, M. S., Dave, A. C., Palter, J. B., Gerber, L. M., and Barber, R. T. (2011). On the relationship between stratification and primary productivity in the North Atlantic. *Geophys. Res. Lett.* 38, eISSN1944–8007. doi: 10.1029/2011GL049414
- Marumo, R., and Asaoka, O. (1974). Trichodesmium in the east China Sea. 1. Distribution of *Trichodesmium thiebautii* gomont during 1961–1967. *J. Oceanogr. Soc. Jap.* 30, 298–313.
- Mills, M. M., Ridame, C., Davey, M., La Roche, J., and Geider, R. J. (2004). Iron and nitrogen co-limit nitrogen fixation in the eastern tropical North Atlantic. *Nature* 429, 292294. doi: 10.1038/nature02550
- Monterey, G., and Levitus, S. (1997). *Seasonal variability of mixed layer depth for the world ocean* (NOAA atlas NRSDIS 14. U. S. Gov. Printing Office).
- Moore, C. M., Mills, M. M., Arrigo, K. R., Berman-Frank, I., Bopp, L., Boyd, P. W., et al. (2013). Processes and patterns of oceanic nutrient limitation. *Nat. Geosci.* 6, 701–710. doi: 10.1038/ngeo1765
- Mulholland, M. R., and Bernhardt, P. W. (2005). The effect of growth rate, phosphorus concentration, and temperature on N₂ fixation, carbon fixation, and nitrogen release in continuous cultures of *Trichodesmium* IMS101. *Limnol. Oceanogr.* 50, 839849. doi: 10.4319/lo.2005.50.3.0839
- Nagai, T., Durán, G. S., Otero, D. A., Mori, Y., Yoshie, N., Ohgi, K., et al. (2019). How the Kuroshio Current delivers nutrients to sunlit layers on the continental shelves with aid of near-internal waves and turbulence. *Geophys. Res. Lett.* 46, 6726–6735. doi: 10.1029/2019GL082680
- Nagai, T., Hasegawa, D., Tsutsumi, E., Nakamura, H., Nishina, A., Senjyu, T., et al. (2021). The Kuroshio flowing over seamounts and associated submesoscale flows drive 100-km-wide 100–1000-fold enhancement of turbulence. *Communic. Earth Environ.* 2. doi: 10.1038/s43247-021-00230-7
- Nan, F., Xue, H., and Yu, F. (2015). Kuroshio intrusion into the South China Sea. *Prog. Oceanogr.* 137, 314–333. doi: 10.1016/j.pcean.2014.05.012
- Nitani, H. (1972). *Kuroshio-its physical aspects*. Eds. H. Stommel and K. Yoshida (Tokyo, Japan: University of Tokyo), 129–163.
- Ohlendieck, U., Stühr, A., and Siegmund, H. (2000). Nitrogen fixation by diazotrophic cyanobacteria in the Baltic Sea and transfer of the newly fixed nitrogen

- to picoplankton organisms. *J. Mar. Syst.* 25, 213219. doi: 10.1016/S0924-7963(00)00016-6
- Pai, S. C., and Riley, J. P. (1994). Determination of nitrate in presence of nitrite in natural water by flow injection analysis with a non-quantitative on-line cadmium reactor. *Inter. J. Environ. Anal. Chem.* 57, 263277. doi: 10.1080/03067319408027460
- Palter, J. B., Lozier, M. S., Sarmiento, J. L., and Williams, R. G. (2011). The supply of excess phosphate across the gulf stream and the maintenance of subtropical nitrogen fixation. *Glob. Biogeochem. Cycles* 25. doi: 10.1029/2010GB003955
- Qu, T., and Lukas, R. (2003). The bifurcation of the north equatorial current in the Pacific. *J. Phys. Oceanogr.* 33, 5–18. doi: 10.1175/1520-0485(2003)033<0005:TBOTNE>2.0.CO;2
- Raimbault, R., Garcia, N., and Cerutti, F. (2008). Distribution of inorganic and organic nutrients in the South Pacific Ocean—evidence for long-term accumulation of organic matter in nitrogen-depleted waters. *Biogeochemistry* 5, 281298. doi: 10.5194/bg-5-281-2008
- Ridal, J. J., and Moore, R. M. (1990). A re-examination of the measurement of dissolved organic phosphorus in seawater. *Mar. Chem.* 29, 1931. doi: 10.1016/0304-4203(90)90003-U
- Saito, H. (2019). “The kuroshio: its recognition, scientific activities and emerging issues,” in *Kuroshio Current: Physical, Biogeochemical, and Ecosystem Dynamics*. Eds. T. Nagai, H. Saito, K. Suzuki and M. Takahashi (AGU-Wiley, Washington, D.C., USA).
- Sarma, V. V. S. S., Rao, D. N., Rajula, G. R., Dalabehera, H. B., and Yadav, K. (2019). Organic nutrients support high primary production in the Bay of Bengal. *Geophys. Res. Lett.* 46, 6706–6715. doi: 10.1029/2019GL082262
- Sato, M., Nishioka, J., Maki, K., and Takeda, S. (2021). Chemical speciation of iron in the euphotic zone along the Kuroshio Current. *Mar. Chem.* 233. doi: 10.1016/j.marchem.2021.103966
- Shaw, P. T. (1991). The seasonal variation of the intrusion of the Philippine Sea water into the South China Sea. *J. Geophys. Res.* 96, 821827. doi: 10.1029/90JC02367
- Shiozaki, T., Takeda, S., Itoh, S., Kodama, T., Liu, X., Hashihama, F., et al. (2015). Why is *Trichodesmium* abundant in the Kuroshio? *Biogeochemistry* 12. doi: 10.5194/bg-12-6931-2015
- Sipler, R. E., and Bronk, D. (2015). “Dynamics of dissolved organic nitrogen,” in *Biogeochemistry of Marine Dissolved Organic Matter*. Eds. D. A. Hansell and C. A. Carlson (Academic Press, Burlington), 127232.
- Sohm, J. A., and Capone, D. G. (2006). Phosphorus dynamics of the tropical and subtropical north Atlantic: *Trichodesmium* spp. versus bulk plankton. *Mar. Ecol. Prog. Ser.* 317, 21–28. doi: 10.3354/meps317021
- Sohm, J. A., Webb, E. A., and Capone, D. G. (2011). Emerging patterns of marine nitrogen fixation. *Nat. Rev. Microb.* 9, 499508. doi: 10.1038/nrmicro2594
- Tang, W., Wang, S., Fonseca-Batista, D., Dehairs, F., Gifford, S., Gonzalez, A. G., et al. (2019). Revisiting the distribution of oceanic N₂ fixation and estimating diazotrophic contribution to marine production. *Nat. Commun.* 10, 831. doi: 10.1038/s41467-019-08640-0
- Tomson-Bullidis, A., and Karl, D. (1998). Application of a novel method for phosphorus determinations in the oligotrophic North Pacific Ocean. *Limnol. Oceanogr.* 43, 1565–1577. doi: 10.4319/lo.1998.43.7.1565
- van de Poll, W. H., Kulk, G., Timmermans, K. R., Brussaard, C. P. D., van der Woerd, H. J., Kehoe, M. J., et al. (2013). Phytoplankton chlorophyll a biomass, composition, and productivity along a temperature and stratification gradient in the northeast Atlantic Ocean. *Biogeochemistry* 10. doi: 10.5194/bg-10-4227-2013
- Wang, S., Xiang, R., Steinke, S., Du, Y., Yang, Y., Wang, S., et al. (2023). Impact of the Western Pacific Warm pool and Kuroshio dynamics in the Okinawa Trough during the Holocene. *Global Planetary Change* 224. doi: 10.1016/j.gloplacha.2023.104116
- Wang, B.-S., and Ho, T.-Y. (2020). Aerosol Fe cyclin in the surface water of the Northwestern Pacific Ocean. *Prog. Oceanogr.* 183. doi: 10.1016/j.pocan.2020.102291
- Wang, Y.-C., and Lee, M.-A. (2019). Composition and distribution of fish larvae surrounding the upwelling zone in the waters of northeastern Taiwan in summer. *J. Mar. Sci. Tech.* 27. doi: 10.6119/JMST.201910_27(5).0008
- Wang, W.-L., Moore, J. K., Martiny, A. C., and Primeau, F. W. (2019). Convergent estimates of marine nitrogen fixation. *Nature*. 566, 205–211. doi: 10.1038/s41586-019-0911-2
- Wang, S.-H., Tsay, S.-G., Lin, N.-H., Hsu, N.-C., Bell, S. W., Li, C., et al. (2011). First detailed observations of long-range transported dust over the northern South China Sea. *Atm. Environ.* 45, 48044808. doi: 10.1016/j.atmosenv.2011.04.077
- Wen, Z., Browning, T. J., Cai, Y., Dai, R., Zhang, R., Du, C., et al. (2022). Nutrient regulation of biological nitrogen fixation across the tropical western North Pacific. *Sci. Adv.* 8. doi: 10.1126/sciadv.ab17564
- Williams, P. J. L. B., and Ducklow, H. (2019). The microbial loop concept: A history 1930–1974. *J. Mar. Res.* 77, 23–81. doi: 10.1357/002224019828474359
- Wong, G. T. F., Chao, S.-Y., Li, Y.-H., and Shiah, F.-K. (2000). The Kuroshio edge exchange process (KEEP) study—an introduction to hypotheses and highlights. *Cont. Shelf Res.* 20, 335347. doi: 10.1016/S0278-4343(99)00075-8
- Wong, G. T. F., Ku, T.-L., Mulholland, M., Tseng, C.-M., and Wang, D.-P. (2007). The South East Asian Time-series Study (SEATS) and the biogeochemistry of the South China Sea: An overview. *Deep Sea Res. II* 54, 1434–1447. doi: 10.1016/j.dsr2.2007.05.012
- Wu, J., Chung, S. W., Wen, L. S., Liu, K. K., Chen, L. Y. L., Chen, H. Y., et al. (2003). Dissolved inorganic phosphorus, dissolved iron, and *Trichodesmium* in the oligotrophic South China Sea. *Glob. Biogeochem. Cycles* 17, 1008. doi: 10.1029/2002GB001924
- Wu, K., Dai, M., Chen, J., Meng, F., Li, X., Liu, Z., et al. (2015). Dissolved organic carbon in the South China Sea and its exchange with the Western Pacific Ocean. *Deep-Sea Res. II* 122, 41–51. doi: 10.1016/j.dsr2.2015.06.013
- Zehr, J., and Capone, D. G. (2020). Changing perspectives in marine nitrogen fixation. *Science* 368, 6492. doi: 10.1126/science.aay9514
- Zhang, Y., Yu, Q., Ma, W. C., and Chen, L. M. (2010). Atmospheric deposition of inorganic nitrogen to the eastern China seas and its implications to marine biogeochemistry. *J. Geophys. Res.* 115, D00K10. doi: 10.1029/2009JD012814